PUERTO RICO NUCLEAR CENTER

F Center Formation at 78°K in KBr During

Exposure to Monochromatic X-Ray Energies

Around the Bromine K Edge

Baltasar A. Cruz Vidal

May 1967

PUERTO RICO NUCLEAR CENTER

F CENTER FORMATION AT 78°K IN KBr DURING

EXPOSURE TO MONOCHROMATIC X-RAY ENERGIES

AROUND THE BROMINE K EDGE

Thesis of

Baltasar A. Cruz Vidal

to

Harvard University

Cambridge, Massachusetts

Work carried out at the

PUERTO RICO NUCLEAR CENTER

under the supervision of

Dr. H. J. Gomberg

MAY 1967

F CENTER FORMATION AT 78°K IN KBr DURING

EXPOSURE TO MONOCHROMATIC X-RAY ENERGIES

AROUND THE BROMINE K EDGE

A thesis presented

by

Baltasar Augusto Cruz Vidal

to

The Department of Physics

in partial fulfillment of the requirements

for the degree of

Doctor of Philosophy

in the subject of

Physics

Harvard University

Cambridge, Massachusetts

May 1967

To Judy

ACKNOWLEDGMENTS

ABSTRACT

In KBr (obtained from the Harshaw Chemical Company) irradiated at $78^{\circ}K$ the rate of formation of F centers per unit energy retained in the crystal was found to be the same whether 13.4 keV or 14.1 keV was the incident photon energy (the K edge of bromine is at 13.5 keV). In other words, at either incident photon energy the energy expenditure per F center formed was 1.21×10^3 eV $\pm$ 4.4%. This result indicates that K shell ionization in bromine does not affect the mechanism of formation of F centers in KBr. However, a large background of multiply ionized atoms is expected whether the incident photon energy is 13.4 keV or 14.1 keV. Each of these atoms becomes multiply ionized after losing an electron in the L shell. Thus, in a bromide the equality of the rate of formation of F centers above and below the K edge is not sufficient evidence to conclude that a Varley mechanism of F center formation is not operative.

Each of the monochromatic beams was the fluorescent output of RbCl filtered with a thin layer of NaBr or of $Sr(NO_3)_2$ filtered with RbCl. The output of a Machlett X-Ray Tube operated at 45 kvp was used to excite the fluorescence. The current in the tube was regulated to achieve the same

energy flux on the sample regardless of the incident photon energy. An air ionization chamber was calibrated with a calorimeter and was used to measure the flux. The half-width of each monochromatic beam was 330 eV.

Measurements of the energy expenditure required to form one F center follow: for KCl (Harshaw Chemical Company) irradiated at 78°K, 6.9×10^{2} eV $\pm$ 4.2%; for KBr irradiated at 300°K, 4.8×10^{3} eV $\pm$ 5.7%; for RbBr (Isomet Corporation) at 78°K, 1.2×10^{3} eV $\pm$ 17%; and for RbBr at 300°K, 1.3×10^{3} eV $\pm$ 30%.

TABLE OF CONTENTS

LIST OF TABLES

LIST OF ILLUSTRATIONS

I. INTRODUCTION

A. Purpose and Motivation for the Study

This thesis succeeds a sequence of studies on the subject of monochromatic X-ray damage in matter.[1-10] These studies were designed to improve the understanding of the mechanism by which ionizing radiation transfers energy to atoms located either in a molecule or in a crystal lattice. The earlier studies were based upon the selective excitation of a metal atom in either a metalloenzyme or in a simpler organic molecule. This thesis has progressed to the excitation of halogen ions in an alkali halide lattice.

Typically, the system under study has been exposed to monochromatic X rays at selected energies in a range which has included an absorption edge of a key atom. Any sensitivity to a change in energy of the incident photons has been determined by observing an important property of either the molecule or the lattice. In some systems an incident energy dependence was observed if the measure of radiation damage had been adequately selected.

Several factors have affected the validity of the

1

results. Paramount to all has been inadequate dosimetry of the beams. The progress experienced in dosimetry has been slow but encouraging. Each previous dissertation has benefited from one more improvement in the accuracy of the dosimetry. The additional difficulty of generating high intensity beams was solved early by the use of fluorescent radiators in combination with thin filters.[11,12] This technique gives an intensity approximately 100 times higher than that possible with a curved crystal monochromator. Also, the early dissertations had been hindered by the fact that the work was done with metalloenzymes of dubious purity and activity and of high sensitivity to extraneous effects such as light and heat.[6] Lately, the systems and the conditions have been improved. Another factor affecting the success of the research has been the choice of a property that will indicate the extent of radiation damage. Indeed, an energy dependence of radiation damage can go undetected if the property being monitored is not closely related to the ionization in the pre-selected atom, or if the property is drastically affected by secondary interactions.

As the work described above progressed, a group at Oak Ridge was increasingly successful in obtaining

ion spectra analysis of the products of inner shell ionization in isolated[13] and in molecular atoms.[14,15] The results of this work have been very useful to the present research program.

The use of alkali halide crystals for research on monochromatic X-ray effects is of particular interest. The crystals, due to their purity and stability, are a great improvement over metalloenzymes and other molecular targets. Also, the research can lead to a better understanding of a fundamental question: During exposure to ionizing radiation, what is the mechanism of formation of vacancies in alkali halide crystals?[16]

The choice of KBr crystals was dictated primarily by limitations of equipment and of techniques. On the one hand, an iodide was not chosen because iodine has an absorption edge close to the maximum voltage output of the X-ray power supply. Consequently, radiators suitable for an iodide irradiation have a low fluorescent output. On the other hand, the K absorption edge of chlorine and the L absorption edge of iodine are too low to use because at these energies the fluorescent radiators would have to be either in vacuum or in a helium atmosphere, and the dosimetry would be particularly difficult. Thus, the convenient energy value of 13.5 keV

for the K absorption edge of bromine made KBr a logical
choice for the primary studies. The availability of high
purity KBr crystals and of a large amount of information
on KBr were additional positive factors influencing the
selection. Also, a second alkali halide, RbBr, was used
in experimentation. The experimental runs on RbBr, as
well as some on KCl, exposed in the energy range of the
K absorption edges of Rb and Br were done to improve the
results of the KBr irradiations. These exposures yielded
information on the energy loss due to fluorescence and
also served as a dosimetry check.

The choice of property to indicate radiation damage
was influenced by the available working temperature, by
the limitations of the spectrophotometer, and by a desire
to make the work relevant to the wide field of existing
research on color centers in solids. The choice was to
monitor the optical F absorption band. Regretfully, the
optical α band[17] was not within the range of accurate
measurement of the optical spectrophotometer, and other
absorption bands[17] were too weak for quantitative
observation. The measurements were taken at room
temperature during the preliminary stages of the work and
primarily at liquid nitrogen temperature as the work
progressed. No other temperatures were available. The

experiment was designed to allow for direct comparison with similar work by J. Sharma who used a curved crystal monochromator.[18]

II. BACKGROUND

A. The Auger Effect

Upon exposure to ionizing radiation, a photoelectron
can be ejected from an inner electron shell. Then, an
atomic electron in a higher energy level can undergo a
transition into the resulting hole. The difference in energy
can be emitted either as a characteristic fluorescent
X-ray photon or, alternatively, as a second electron from
the higher energy level. The latter process is the
Auger effect. A combination of fluorescent and Auger
cascades can bring the electron deficiency to the
outermost shells. As a hole proceeds from the K to the L
to the M shells, the Auger transition becomes much more
probable than a fluorescent transition. Thus, an inner
shell ionization can lead to a high degree of ionization in
an atom and could be important in the analysis of radiation
damage. The basic work on the Auger effect has been reviewed
in a monograph by E. H. S. Burhop.[19] Therefore, the present
review of this phenomenon is limited to recent work which is
directly relevant to the subject of this thesis.

Approximately ten years ago, Snell and Pleasonton
recorded the charge spectra of gas atoms that had undergone

6

internal conversion or electron capture involving an inner shell electron.[20-24] Later, Carlson and White studied the ionic charge distribution that followed similar radioactive decay in a molecular atom.[25-29] Under Carlson, Krause, White, and co-workers, the work progressed to an analysis of the charge distribution that follows an initial inner shell ionization in rare gases,[30-33] in heavier atoms,[13] and in simple molecules.[14,15] Furthermore, the enhancement of ionization which is due to electron shakeoff following either the beta decay of rare gas isotopes[34-36] or the K shell ionization of neon[37] was calculated. A summary of the work on the X irradiation of atoms; a derivation of empirical rules for estimating the total ionization after inner shell ionization of atoms; and a brief discussion of the similarities of multiple ionization in isolated atoms, in molecular atoms, and in lattice atoms were reported. Figures 1 and 2 are from that report.[13]

The Auger cascade proceeds within a molecular atom and is independent of other molecular atoms until the holes reach the outer shells. Then, complex non-radiative processes involving interatomic transfer of either electrons or excitation can take place. Similarly, the initial stage of a hole cascade in a condensed medium is expected to proceed while localized at one atomic site. In the outer shells electron transfer and further autoionization can occur. Presumably,
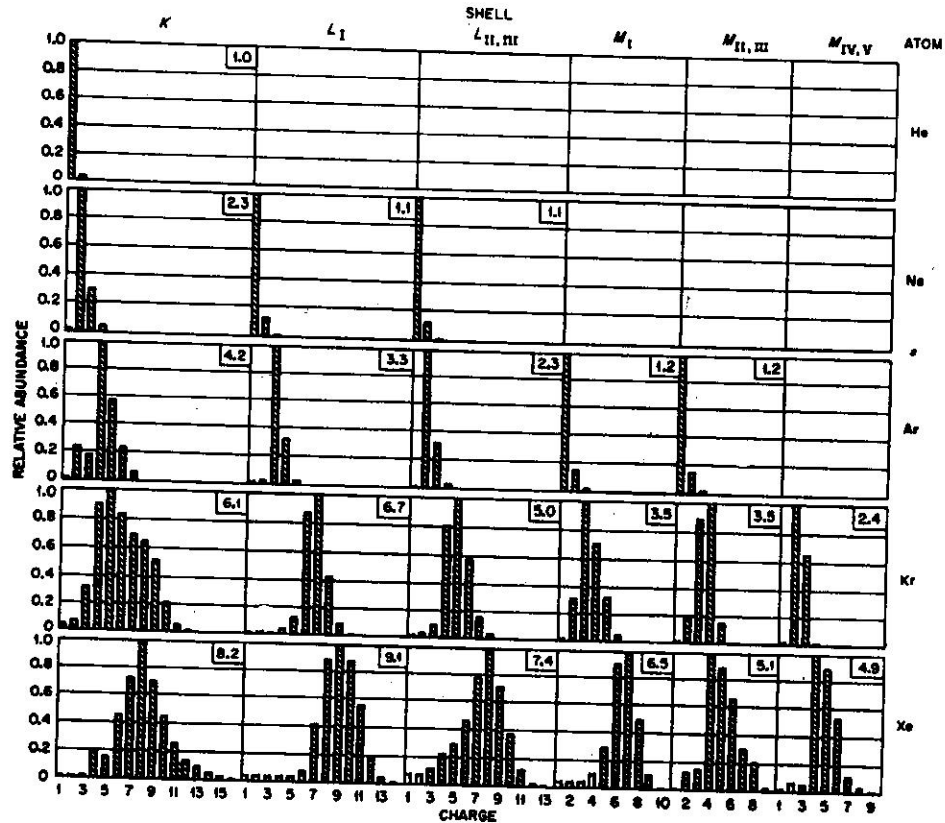
Figure 1. "The relative abundances of ions that are formed as the consequence of a sudden vacancy in a K, L, or M shell of the rare gases. The average charge is given for each spectrum in the upper right-hand corner. The bars containing a notch on top represent an upper limit to the designated intensity." After Carlson, Hunt, and Krause, reference 13.
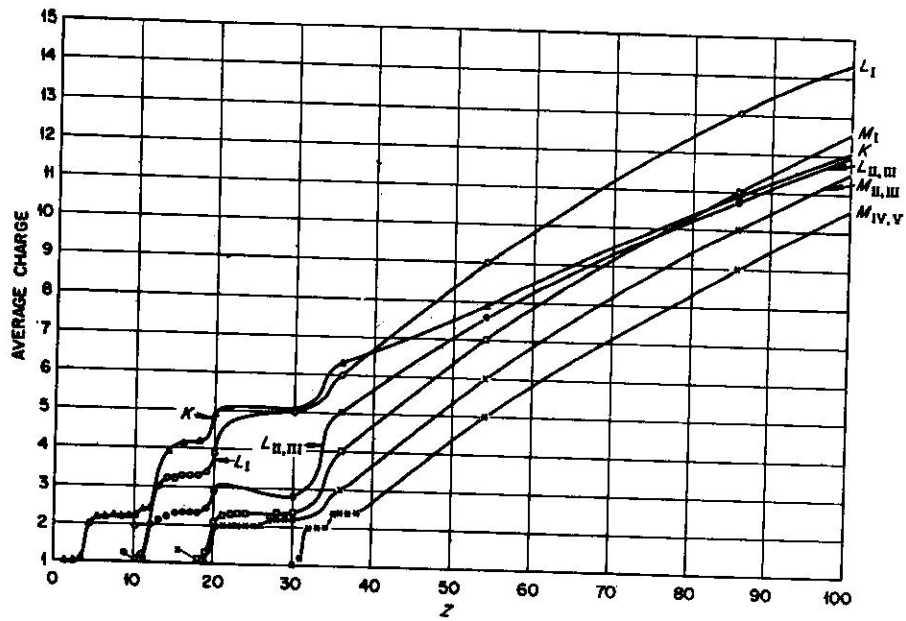
Figure 2. "Estimated average charge as the result of a sudden vacancy in a K, L, or M shell as a function of the atomic number." After Carlson, Hunt, and Krause, reference 13.

in metals effective neutralization can take place as each hole appears in the conduction band.[13] On the other hand, the extent of ionization in a halogen ion of an alkali halide lattice depends on the time required for electron-hole recombination. This question was discussed by several research workers. They estimated a time of the order of 10^{-13} seconds for recombination.[38-42] Since the Auger cascade in one atom takes place in a time of the order of 10^{-15} seconds[13]; then, in an alkali halide lattice, an Auger cascade should proceed unhindered until the holes appear in the outermost ionic shells.

Using Figure 2 one can estimate that a chlorine ion in an alkali halide lattice would lose, on the average, either 3.3 electrons if it is ionized in the L_I shell or 4.2 electrons if it is ionized in the K shell. According to a computer calculation by L. T. Chadderton formation of Frenkel defects can occur following this degree of ionization of a chlorine ion in a KCl lattice.[43]

On the basis of the ionic explosion observed by Carlson, Krause, and co-workers, one can expect that in some molecules or solids--if the measure of radiation damage is adequately selected--one would observe damage arising from an ionic explosion that follows inner shell ionization of a particular atom.

B. Radiation Damage in Molecules

R. L. Platzman first pointed out the possible role of the Auger effect in radiation damage to biological systems.[44] Later, its possible relevance to the creation of vacancies and interstitials in alkali halides was recognized by J. Durup and R. L. Platzman,[45] and by R. Smoluchowski and D. A. Wiegand.[46] However, the thorough work of Snell, Carlson, Krause, and co-workers on the Auger effect had gone largely unnoticed by researchers in the field of radiation interaction with matter. H. J. Gomberg recognized the significance of Snell's early results and suggested that certain molecules can undergo radiation damage by means of a mechanism which is dependent on the incident photon energy. For example, an organic molecule is usually composed of low atomic weight atoms; but if it also contains one or a few medium weight atoms, absorption of energy in an inner shell of one of them should lead to massive molecular damage more efficiently than absorption of energy elsewhere. In this case, an Auger cascade would follow the inner shell ionization and would lead to the formation of a multiply ionized ion. Molecular breakup would be likely to occur at the site of the multiple ionization. The mechanism described above is called the sensitive site hypothesis of radiation damage. Of

significance is the known fact that in several biologically
important molecules, such as metalloenzymes, a relatively
heavy metallic atom is incorporated into a structure that
is essential to the performance of the biochemical function
of the molecule. A molecular breakup at the metallic atom
site would be particularly effective in inhibiting the
biochemical function of the molecule and, therefore, should
provide a fairly direct measure of radiation damage.
However, to verify the sensitive site hypothesis of
molecular damage would be a difficult experimental problem.
For example, the molecule should be stable at the
temperature of observation, and the test of sensitivity
should be straightforward. Also, any observed effect would
be dependent on the ratio of sensitivity-to-damage by the
primary event to sensitivity-to-damage either by secondary
radiation or by primary radiation on all other molecular
sites.[1-10]

The completed problems and experiments on
monochromatic damage in molecules under Gomberg's direction
were the subject of a series of doctoral dissertations at
the University of Michigan[1-7] and of further research at
the Puerto Rico Nuclear Center.[8-10] One main difficulty in
this area of research was adequate control of the experiment.
For example, the selective excitation of a particular
energy level within a particular atom requires the use of

monochromatic X rays. Beams of high intensity and accurately known energy fluxes must be used. The early work at Michigan[1,2] had been completed before the necessary techniques were fully developed. Since then, the techniques have increasingly improved.[11,12]

Reviews of previous work on radiation damage in molecular systems were included in the dissertations by A. H. Emmons[2] and by M. C. Atkins.[3] P. Paraskevoudakis, in his dissertation, pointed out the difficulty in working with metalloenzymes, such as catalase, of dubious activity and purity and of troublesome dependence on light and temperature. Likewise, he focused attention on the difficulties in calibrating dosimeters in experiments run in the soft X-ray region. Also, he reviewed the results which were published in the series of experimental theses mentioned above. Thus, his thesis provides a valuable analysis of both the techniques used in this research and the results.[6]

The studies by Emmons,[2] by Paraskevoudakis,[6] and by R. A. Luse[8,9,10] indicated an increased efficiency of radiation damage in the enzyme catalase when it had been exposed to radiation that is preferentially absorbed in the iron atoms of its porphyrin ring structure. In this case, the measure of radiation damage was the decrease in activity of the enzyme as indicated by the reduction of

hydrogen peroxide. However, the work of W. R. Clendinning on the free radical yield in 1-bromobutane, as measured by reaction with DPPH, showed no unique dependence on incident energy.[4] Similarly, the experiments by Atkins on the metallic yield of a pure organic mercury compound that had been exposed to X-ray photons in the region of the mercury L absorption edges showed no particular energy dependence.[3] On the other hand, the thesis by Paraskevoudakis on the inactivation of horseradish peroxidase (an enzyme which is similar to catalase and also contains iron in a porphyrin ring structure, but which is less sensitive than catalase to light and temperature) indicated that when the enzyme had been exposed to photon energies above the K absorption edge of iron, a greater decrease in enzymatic activity occurred than when the incident energy had been below the K absorption edge. Also, for incident photon energy above the K absorption edge an apparent increase in the breakup rate of the porphyrin ring was observed optically.[6]

The work by F. S. Koo on onion-root tip cell chromosomes which had been incorporated with 5-bromodeoxyuridine indicated that there was an increased incidence of chromosome breakage when the cells had been exposed to photon energies above, rather than below, the K absorption edge of bromine.[10]

From the work on monochromatic radiation damage in

biological systems, some basic concepts have emerged:
First, selective absorption of radiation in a particular
atom leads to a measureable change in a property under
observation if the selectively excited atom is analogous
to an impurity in a molecular structure composed mainly of
lower weight atoms. Second, the selectively excited atom
must play a significant role in the property which is under
evaluation. Third, the molecule must not be extremely
sensitive to secondary radiation effects. Finally, if the
number of molecules damaged per incident photon is very
large, the gross radiation effect will dominate.

The excitation of a halogen ion in an alkali halide
lattice does not fully meet the requirements stated above.
Therefore, only the scientist's lack of knowledge of the
mechanism of formation of defects during irradiation
provides the driving incentive for experimentation such
as that described in this thesis.

C. Radiation Damage in Alkali Halide Crystals

1. Color centers in irradiated crystals

Much available information about colored crystals,
particularly about alkali halides which had been colored by
exposure to ionizing radiation, has been collected in two
recent monographs.[47,48] Thus, the present review is

limited to basic information which is essential to the understanding of this thesis and to recent information which was not included in the monographs.

The absorption spectra of alkali halides which have been exposed to ionizing radiation are composed of characteristic absorption bands in the range from the fundamental absorption edge to the near infrared.[17] See Figure 3.[49] The F band is best known. It appears in the visible region and is stable at room temperature. Electron paramagnetic resonance studies on F colored crystals showed that the presence of an F band is due to the absorption of light by an electron located in a halogen ion vacancy. The F center can be formed by exposing an alkali halide crystal to ionizing radiation or to ultraviolet light.[50]

Other bands, such as the α, the H, the V_K, the V_1, and the V_2 bands, are of great importance to the understanding of radiation damage in alkali halide crystals. These bands are stable at low temperatures (5°K to 78°K) and are generated, together with the F band, by ionizing radiation.

The α and the β bands are the most prominent of those found on the shoulder of the fundamental absorption edge. The α band is due to the formation of an exciton next to a halogen ion vacancy. The β band, which appears on the high energy side of the α band, is due to the formation of an exciton
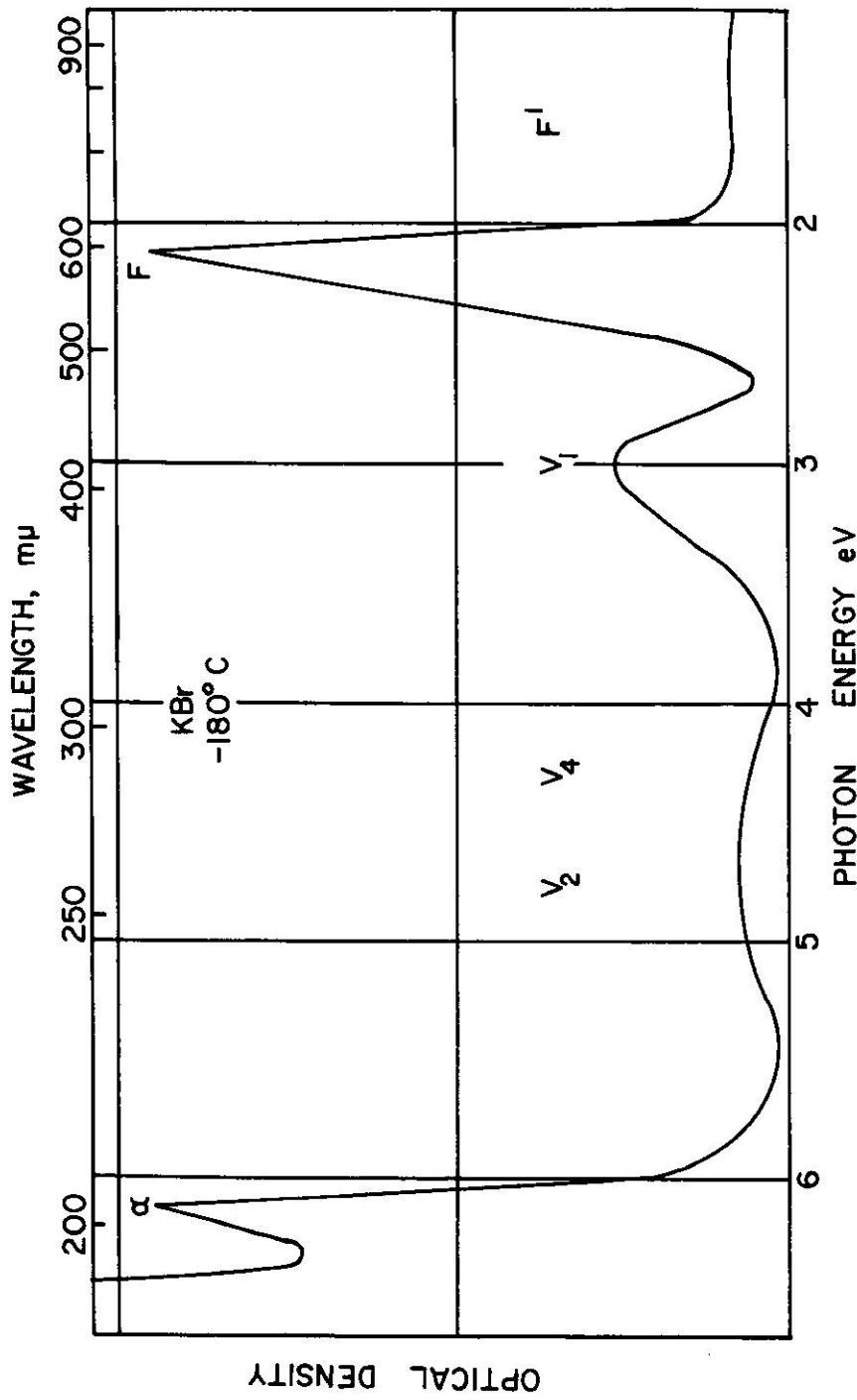
Figure 3. A typical absorption spectrum of KBr after exposure to X rays. The most prominent bands are labeled. After Schulman and Compton, reference 49.

located near an F center.

Light absorption near the region of the α and the β bands can be observed when impurities, such as thallium ions or hydroxyl ions, are present in a crystal. This absorption can be great enough to obscure the α and the β bands and to distort the fundamental absorption edge. As the wavelength is increased, a whole series of temperature dependent absorption bands can be observed in irradiated crystals. These bands are called the V bands and the H band. Impurities acting as either electron or hole traps can alter the stability of some of these bands.[51]

The optical H band bleaches thermally at a temperature below 78°K which is characteristic of the particular alkali halide observed. This thermal bleaching leads to the growth of another optical band, the V_1 band. Electron paramagnetic studies indicated that the H band results from the substitution of a (halogen)$_2^-$ molecular ion for a negative halogen ion in the lattice. Thus, the center responsible for the H band is the chemical equivalent of a neutral halogen interstitial. Recombination of an H center with an F center would return the lattice to the virgin state. In Figure 4 the structure of an H center is shown.

The optical V_1 band, in KCl, KBr, and LiF, is not due to a paramagnetic center. The structure of the
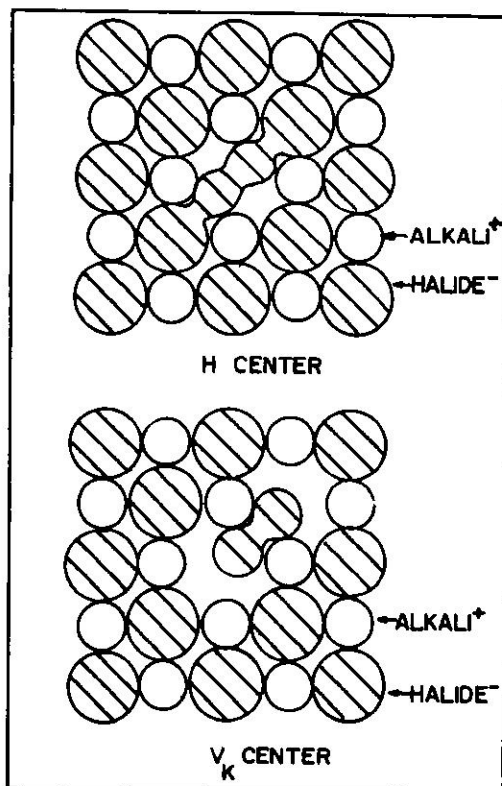
Figure 4. Models of the H center and of the V_K center. The ratio of the ionic radii shown is that of KCl. After Kanzig and Woodruff, reference 52.

V_1 center is not fully understood, but its bleaching properties suggest that it is similar to the H center.[52]

The V_2 band was recently studied in KI which had been exposed to either ultraviolet light or X radiation. The efficiencies of formation of both the V_2 and the F bands increased rapidly to a maximum as the temperature rose from $78^{\circ}K$ to $130^{\circ}K$; then, they decreased slowly as the temperature increased to $180^{\circ}K$. This behavior suggests that there is a relationship between the structures of the F and the V_2 centers. Possibly, the V_2 center is a halogen center which is complementary to the F center in this temperature range. Hersh suggested that an interstitial I_3^- molecule is a possible model for the V_2 center. This model is consistent with present optical knowledge of iodide crystals and iodine solutions, and with the observed absence of paramagnetism due to the V_2 center. The importance of the V_2 center in KI arises from the fact that the V_2 center and the F center have efficiencies of formation which have a similar dependence on temperature.[53] This fact, as well as the fact that the luminescence during irradiation changes with temperature, led to a reasonable hypothesis for an excitonic mechanism of F center formation.[54-57]

Upon X irradiation of impure crystals a strong impurity dependent band, the V_K band, appears in the

V_1 region. Its appearance can obscure the V_1 band. The V_K center was identified by its electron paramagnetic signal as a self-trapped hole in the field of two adjacent halogen ions. The chemical structure of the V_K center is similar to but its lattice geometry differs from that of the H center. See Figure 4. In pure KI crystals the V_K center is unstable. To stabilize it an electron trapping impurity seems necessary. However, the intrinsic luminescence which was observed during irradiation of pure KI was identical to that arising from optical excitation of the V_K center in less pure KI crystals. This fact indicates that the V_K center exists as a transient during X irradiation of pure KI.[53]

Exposure of alkali halide crystals to X rays brings about formation of the whole spectrum of ultraviolet and visible bands, which have been described above. Other less prominent bands are also formed. Many optical bands have a peculiar temperature dependence which is of great importance to the scientist's understanding of the configuration, the stability, and the formation of their corresponding centers.

2. Growth curve of the F band

During irradiation at room temperature the optical absorption at the maximum of the F band follows two stages.

First, rapid coloration occurs. Second, a gradual increase in the coloration takes place. The initial rapid coloration, which corresponds to a fast increase in the density of F centers, is attributed to the filling of available halogen vacancies.

Even in the best crystal, to satisfy thermodynamic considerations vacancies must be present.[58] Vacancies are also caused by numerous dislocations which are always present in a crystal. The density of vacancies is increased by the presence of impurities because the impurities imperfectly fit the lattice and/or because electrical neutrality must be maintained. At room temperature the actual concentration of vacancies in a crystal which is suitable for optical research has been estimated to be from 10^{15} to 10^{17} vacancies per cubic centimeter.[59]

At room temperature the presence of hydroxyl ion impurity enhances the early stage colorability of a crystal that is exposed to radiation.[59]

Particularly, at low temperature the presence of impurities capable of providing electron and/or hole traps can affect: the stability of trapped-hole centers, especially the V_K center; both the intrinsic and the thermal luminescence; and the efficiency of formation of F centers.[53,60-66]

The work of Rabin and Klick at 5°K supports the

two-stage growth curve of F band coloration. They found
that during a second irradiation crystals which had been
colored and bleached required an energy expenditure of
28 eV per F center formed. The same crystals had required
2000 eV per F center formed during the original irradiation.
The early stage coloration at room temperature had been
found to require approximately 30 eV per F center formed.[67]

Rabin and Klick's work showed that there is a lack
of dependence of F center formation on impurity and
dislocation concentrations at $4^\circ K$ and at $78^\circ K$,[67] while at
room temperature the dependence on impurity, observed by
Etzel, is significant.[59] However, in view of present
knowledge the roles of impurities, including their effect
as electron and/or hole traps at various temperatures,
should receive further attention. Apparently, the region
of low temperature, where impurities are not very important,
can be considered to be below the temperature range in
which thermal reorientation of the V_K center and other
trapped hole centers occurs. The location of this range
may depend on the type of impurity present in the crystal.
Clearly, the roles of impurities are of great interest.[53,60-66]

Rabin and Klick found that the energy of formation per
F center is dependent on the lattice parameter of the
crystal. They suggested that the displacement of an ion
depends on the space available for the ion in an

interstitial position.[67]

Available evidence indicates that the F and the H centers are formed at $5^\circ K$[68] by a process which is independent of impurity and dislocation concentrations, but which is dependent on the lattice parameter.[67] As seen in Figure 4, the H center is an interstitial halogen atom in a crowdion configuration.[52] That is, it is the center whose recombination with the F center would restore the crystal to its virgin state. Therefore, one can postulate that the basic mechanism of formation is the same for the α and the F centers, as well as for the H, the V_1, and the V_2 centers. Namely, a halogen ion is displaced from its lattice position and moves into either a crowdion or an interstitial configuration that, depending on the temperature, will then give rise to an H, a V_1, or a V_2 center. The resulting halogen ion vacancy has a certain affinity for the electrons that are created by the radiation. Thus, some of the vacancies capture electrons to form F centers, while others remain as α centers.

The actual mechanism leading to displacement of the halogen ion requires further study. To add to the body of information on this subject is a goal of this dissertation. The models for the mechanism of production of color centers have been reviewed by Schulman and Compton.[16] However, for the sake of completeness the literature on this

subject will be reviewed here also.

3. The Seitz mechanism of F center formation--a Schottky defect mechanism

A mechanism of forming F centers that involves the formation of interstitials differs noticeably from the mechanism proposed by F. Seitz. Seitz postulated that the simultaneous generation of positive ion vacancies and negative ion vacancies occurred by means of the climb of dislocation lines. Meanwhile, vacancy pairs formed which then diffused away from the dislocation until they were trapped by an electron and dissociated.[69,70] See Figures 5 and 6.[71]

The Seitz mechanism was proposed to explain why an increase in ionic conductivity is observed in a plastically deformed alkali halide crystal. Since this increase in ionic conductivity caused by the deformation gradually decreases, he postulated that neutralization of these vacancies would occur due to their accumulation, preferably near dislocations, as immobile clusters. Free electrons, holes, and excitons which are all generated by X radiation, as well as excitons which are generated by ultraviolet light, would have a solvent action on the clusters of vacancies that would be present in the crystal. At room temperature a plastically deformed alkali halide crystal
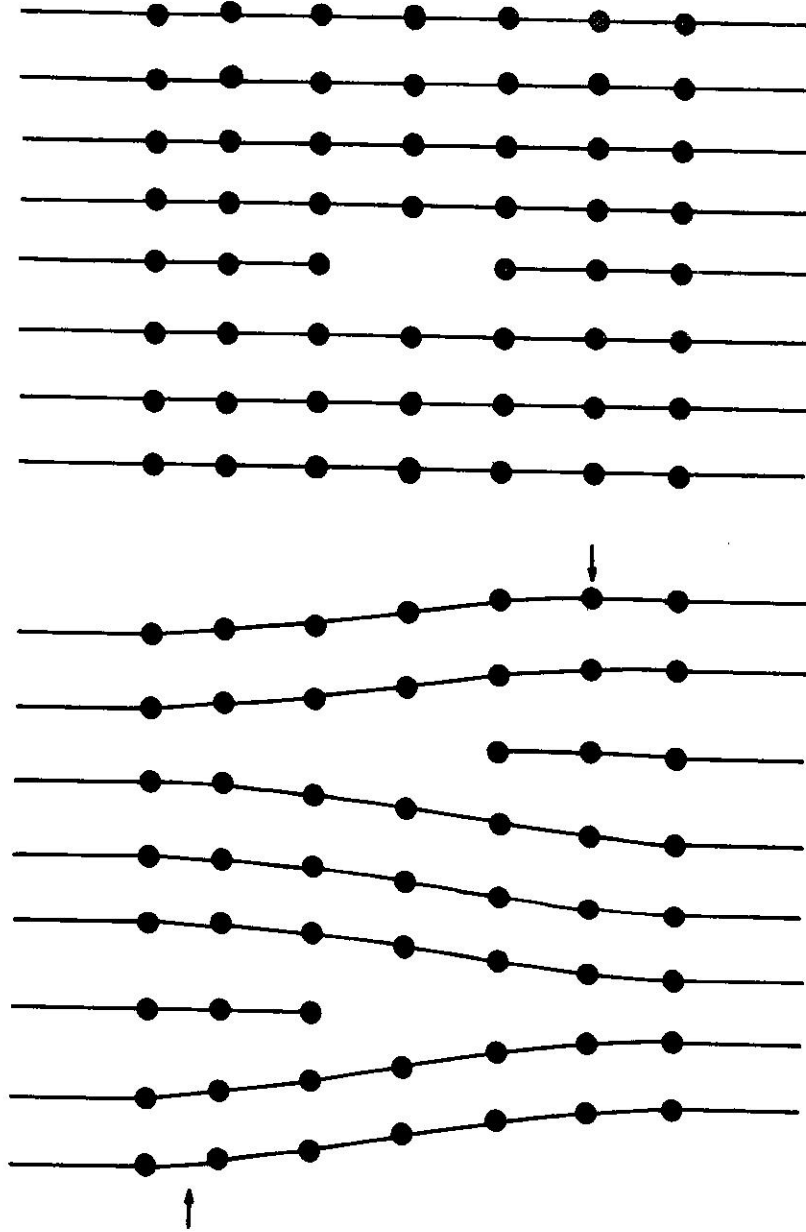
Figure 5. "Formation of a row of vacancies by the intersection of two edge dislocations separated by one atomic distance." After Schulman and Compton, reference 71.
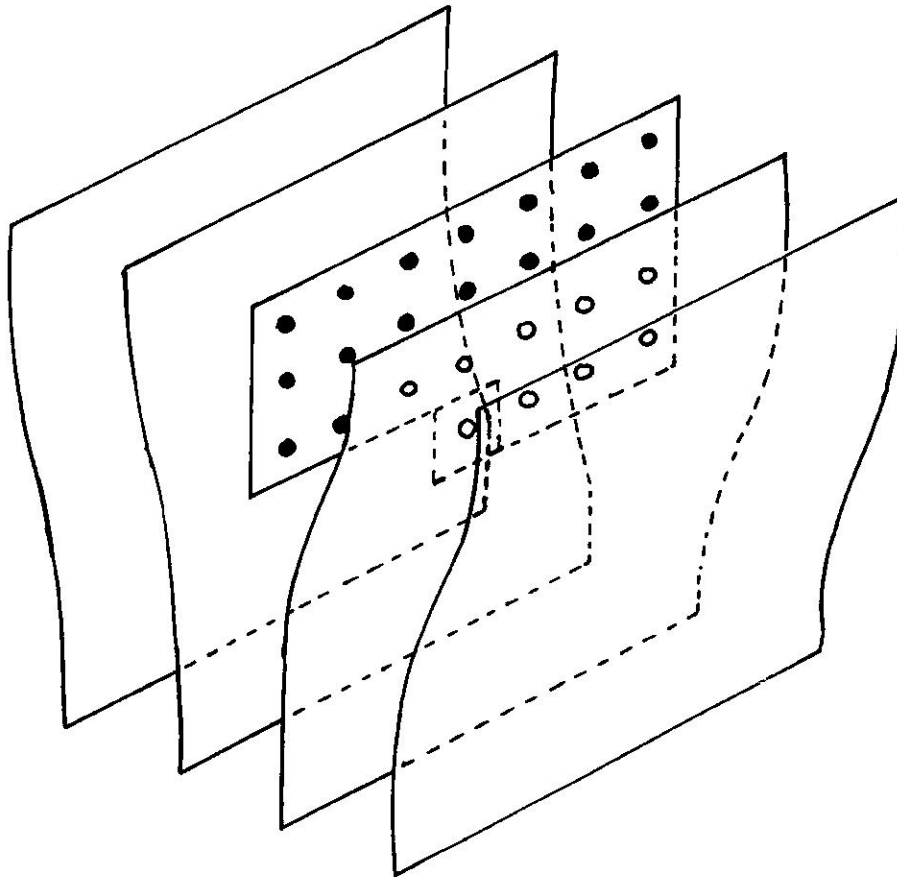
Figure 6. "An edge dislocation with one jog in it. Only one family of lattice planes is shown, and atoms are shown on only one of these planes, the incomplete one. If the atom enclosed in the small square diffuses away, the jog moves one place to the right. This and its reverse are the elementary processes of climb." After Schulman and Compton, reference 71.

to the concept that Schottky defects were formed in crystals. But so far, the absence of well-controlled experiments which involve measurements of volume expansion and change in lattice parameter of the same crystal has hindered interpretation of the results. However, H. Peisl recently reported simultaneous measurements of lattice parameter and volume expansion of KCl which indicated that Frenkel defects (vacancy-interstitial pairs) are formed during X irradiation at room temperature.[85]

4. Mechanism for
the formation of
Frenkel defects

As early as 1954 J. H. O. Varley postulated that Frenkel defects are formed in a perfect lattice during irradiation. According to his original proposal, incident radiation would ionize the negative halogen ion at least twice by means of a photoelectric interaction. The resulting positive halogen ion would be unstable in its normal lattice position. Therefore, it would be displaced by the electrostatic force and thermal vibration or its own recoil energy. At low temperatures the positive halogen would come to occupy an interstitial position where it would be neutralized and would become an H center.[86-88]

In 1958 W. Kanzig identified the H center at 4°K as essentially a halogen atom interstitial which is

complementary to the F center in a Frenkel defect.[52]

Later, H. Rabin and C. C. Klick concluded that at $4^{\circ}K$ vacancy formation is independent of factors that affect the perfection of the lattice but is dependent on the lattice parameter in a way which suggests that the space available for an interstitial is significant to vacancy formation.[67]

At liquid helium temperature KBr has an α band that corresponds to a vacancy concentration which is about 6 times larger than the F center concentration.[92-95] Accordingly, from the energy of formation of 2×10^3 eV per F center,[67,96] one calculates an energy of formation per vacancy of about 3×10^2 eV. By assuming that ionization occurs only in the valence shells, with a probability of 1/2 for a first ionization and of 1/10 for a second ionization, and by assuming a band gap of 10 eV, one can estimate that about 2×10^2 eV would be required if every double ionization were to lead to a vacancy. This value agrees with the experimentally derived energy of formation of 3×10^2 eV per vacancy.

Thus, the basic evidence supporting a mechanism of Frenkel defect formation can be summarized as follows: At liquid helium temperature interstitials were identified.[52,89-91] At this temperature the rate of formation of F centers is largely independent of the history and the purity of the crystal but is dependent on

the lattice parameter.[67] Furthermore, the Varley mechanism is reasonable when the energy requirement for vacancy formation is considered. Also, the fact that Frenkel pairs are formed during X irradiation at room temperature has been verified.

On the basis of a tightbinding approximation, R. E. Howard and R. Smoluchowski estimated that in a typical soft X-ray irradiation the period of time which ions need in order to capture electrons from the conduction band is of the order of 10^{-12} seconds.[38] This time estimate is sufficient to allow for the displacement of a doubly ionized halogen by electrostatic forces--as required by the Varley mechanism. However, by using a band approximation and by assuming a free electron mass for the two holes in a doubly ionized halogen ion, D. L. Dexter estimated that the holes would separate by one interionic distance in 10^{-15} seconds. This neutralization time of the halogen ion is shorter than the displacement time that is required by the Varley mechanism. Dexter's objection to the Varley mechanism was that the time before neutralization is too short to allow for ionic displacement by the electrostatic force.[39]

In response to Dexter's objection, C. C. Klick proposed that the capture of one electron by the twice ionized halogen, instead of neutralizing the Varley mechanism, would lead to the formation of a halogen molecule.

The halogen molecule would be localized at one lattice site. After several jumps the molecule would be separated from its vacancy, and each would be free to capture an electron.[97]

Any functioning mechanism of Frenkel defect formation must lead to a separation of the vacancy from the interstitial. At low temperatures simple diffusion as required by the Klick mechanism cannot account for this separation. In fact, N. Itoh showed that in KBr at 4^OK interstitial diffusion is very low or nonexistent.[74] Therefore, at liquid helium temperature the process of diffusion in Klick's mechanism is problematical.

Smoluchowski estimated (private communication) that the small fraction (about 1/6 in KBr) of the o centers which are formed at 4^OK and which survive warming to 78^OK are stabilized because they are located close to an interstitial, to an impurity, or to a dislocation--each of these effectively repels electrons. Smoluchowski's view is consistent with the observation that most vacancies at low temperature are located far from an interstitial. For example, the separation between the H and the F centers must be large since no interaction was observed between them in the electron spin resonance experiments of W. Kanzig[52,98] nor in the polarized light experiments of W. D. Compton and C. C. Klick.[99] Likewise, measurements of J. D. Konitzer and

J. J. Markham of optical absorption bands showed neither displacement nor broadening of the bands, which indicates an absence of interaction with nearby centers.[100] After a careful study of the recombination stages of vacancies with interstitials in KBr, N. Itoh concluded that an interstitial and its corresponding vacancy are probably separated by approximately 10 lattice spacings.[101]

R. E. Howard, S. Vosko, and R. Smoluchowski recognized that approximating the hole mass by the free electron mass, as well as making a band approximation, results in an underestimate of the period of stability of multiple ionization in a lattice ion. They also noticed that the period of time before electron capture occurs would be long enough to allow a molecular attraction between the doubly ionized halogen and its neighboring halogen ion. In the case of KCl, they postulated that the positive and the negative halogen ions would approach each other and that when they were close, a transition to a repulsive state of the Cl-Cl configuration would be possible. In the presence of the repulsive force one of the halogen atoms would be displaced. They estimated the kinetic energy given to a displaced halogen atom to be 3 eV. This energy would be sufficient to further displace the atom by several lattice spacings. In its new position the displaced atom would become an interstitial, an H center. The leftover

vacancy and the other halogen atom would capture electrons.[40]

On the basis of a tight binding approximation in an alkali chloride, F. E. Williams calculated that if adjacent halogen ions were singly ionized, then the time required for hole separation to occur would be (3×10^{-14} seconds) of the same order of magnitude as the time required for Cl_2^- to form from one of the ionized halogens and a neighboring negative halogen ion. The polarization field which would be produced by the second hole that would be located nearby the molecular ion would impart 1.1 eV to the molecular ion. This would be enough to separate the Cl_2^- molecular ion (H center) from its corresponding vacancy, which would then be free to capture an electron.[41]

Also, Williams stated that in some antisymmetric states momentum could be imparted to isolated Cl_2^- centers during formation of the molecular ion. This action would lead to an inefficient process of vacancy-interstitial separation, but he considered this process to be reasonable in view of the high probability of forming isolated Cl_2^- molecular ions.[41]

5. Formation of F centers
in crystals exposed
to ultraviolet light

In England a group of scientists succeeded in

inducing coloration in pure potassium iodide crystals,[102] as well as in pure potassium bromide crystals,[103] by exposing them to ultraviolet photons of energies that corresponded to the crystals' respective β absorption bands. Similar work done in the United States was successful in inducing coloration that was due to F centers and V aggregate centers in pure KI.[53]

J. D. Gibson and co-workers did computer calculations on the formation of defects which occurs during neutron irradiation of copper crystals. They showed that a replacement sequence can lead to Frenkel defect formation.[104] The formation of Frenkel defects in alkali halide crystals during ultraviolet or X irradiation was recently studied by applying computer calculations similar to the ones used by Gibson. The results indicated that Frenkel defects in alkali halides can be formed by a low energy mechanism. H. E. Hersh suggested that the source of energy for the replacement sequence would be an exciton whose hole is captured in a V_K center.[54-57] The energy of recombination of the electron and the hole of the V_K center would be the source of energy for the replacement sequence. Furthermore, Hersh suggested that an alternative mechanism can occur--a lattice relaxation by means of the emission of luminescence.[54] Hersh's suggestions are supported by the observation that

the efficiency of F center formation during X irradiation increases in the same temperature region in which the exciton luminescent intensity decreases.[53,105-107] This is the temperature range in which thermal disorientation of the V_K center also occurs.[108,109]

The initial event in the low energy mechanism of formation of F centers requires only 6 eV, but the mechanism may be inefficient.[103] Thus, the observation that the energy of formation of F centers is of the order of 2000 eV per F center can be justified. However, there is no evidence to indicate that a low energy mechanism is the only possible source of Frenkel defects. In fact, the computer calculation by Chadderton suggested that multiple ionization of a halogen atom can lead to formation of Frenkel defects. For example, the calculation showed that triply or quadruply ionized chlorine in KCl can undergo focused collisions, in either the <111> or the <110> direction, which lead to Frenkel defect formation. After a collision in the <111> direction the formation of a stable defect would require some thermal activation. Thus, a temperature dependence can be built into this model. Chadderton's work indicated that single or double ionization of chlorine in a KCl lattice would not lead to Frenkel defect formation, but that a higher degree of ionization of chlorine in KCl would lead to Frenkel defect formation.[43] Carlson and

Krause demonstrated that after a K or an L_I shell ionization in chlorine, the loss of three or four electrons is more likely to occur than the loss of one or two electrons. Thus, the conditions that the computer model requires for Frenkel defect formation are likely to occur in the typical X-irradiation experiment. See Figures 1 and 2.[13]

III. EXPERIMENTAL METHOD AND RESULTS

A. The Monochromatic X-Ray Source

The primary X-ray source was a General Electric XRD-5 unit, which is pictured in Figure 7. This unit is capable of operating at up to 50,000 volts and at up to 50 milliamperes. During the course of the work several Machlett AEG-50 tungsten target tubes were used.

Figure 8 is a schematic diagram of the method which was used to produce monochromatic X rays. The output from the X-ray tube irradiates a radiator which fluoresces. As long as the X-ray tube is operated above the K absorption edge of the element in the radiator, the fluorescent output of the radiator consists primarily of the K_α and the K_β emission lines of this element. The output is filtered by a thin film that contains an element whose K absorption edge lies between the respective energies of the K_α and the K_β lines. The K_β radiation, being of higher energy than the K_α radiation, is preferentially absorbed by this filter. The filtering action is illustrated in Figure 9. The K_α intensity available after filtration is significantly higher than the intensity obtainable using a curved crystal monochromator.
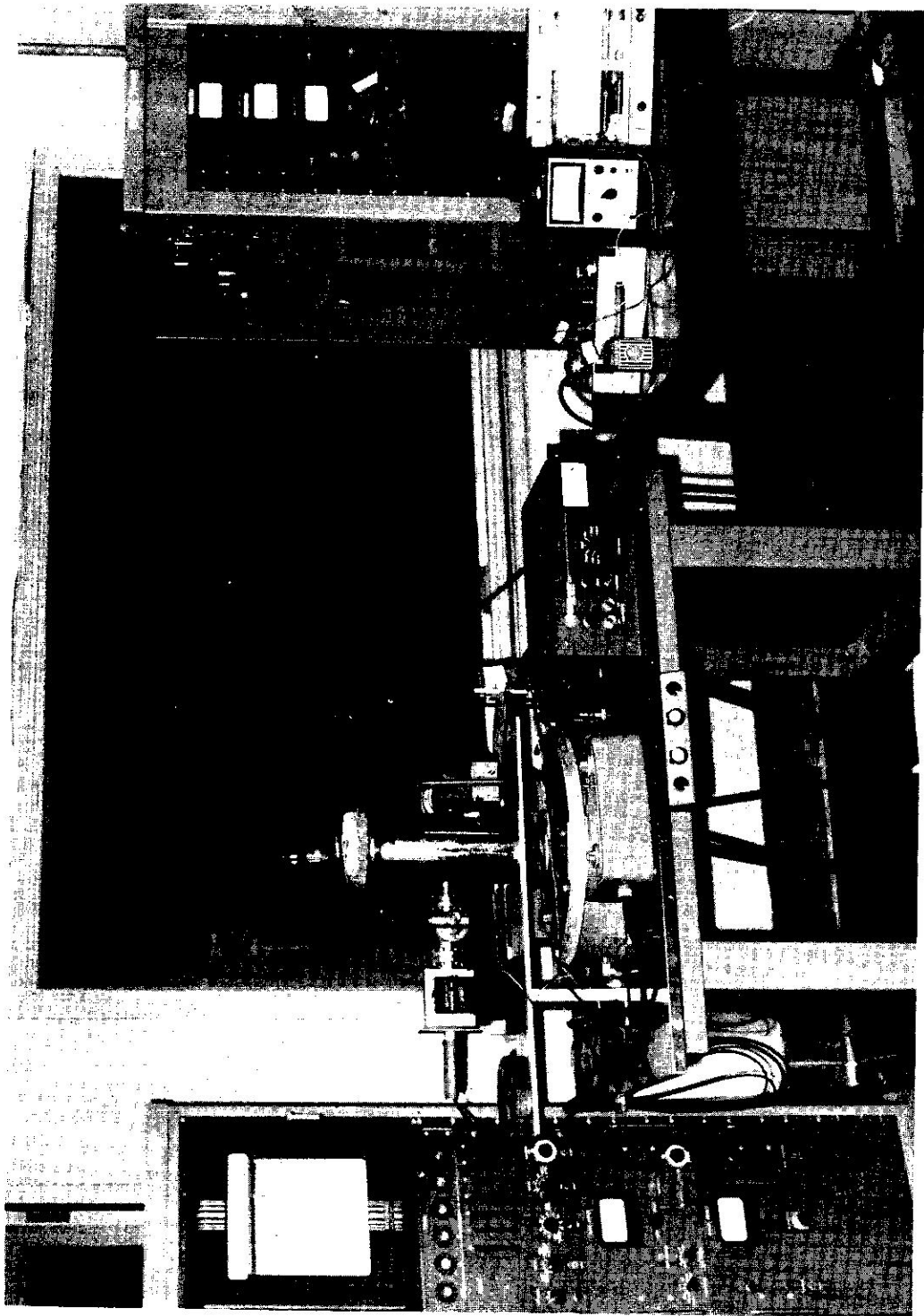
Figure 7. The General Electric XRD-5 X-ray Diffraction Unit.
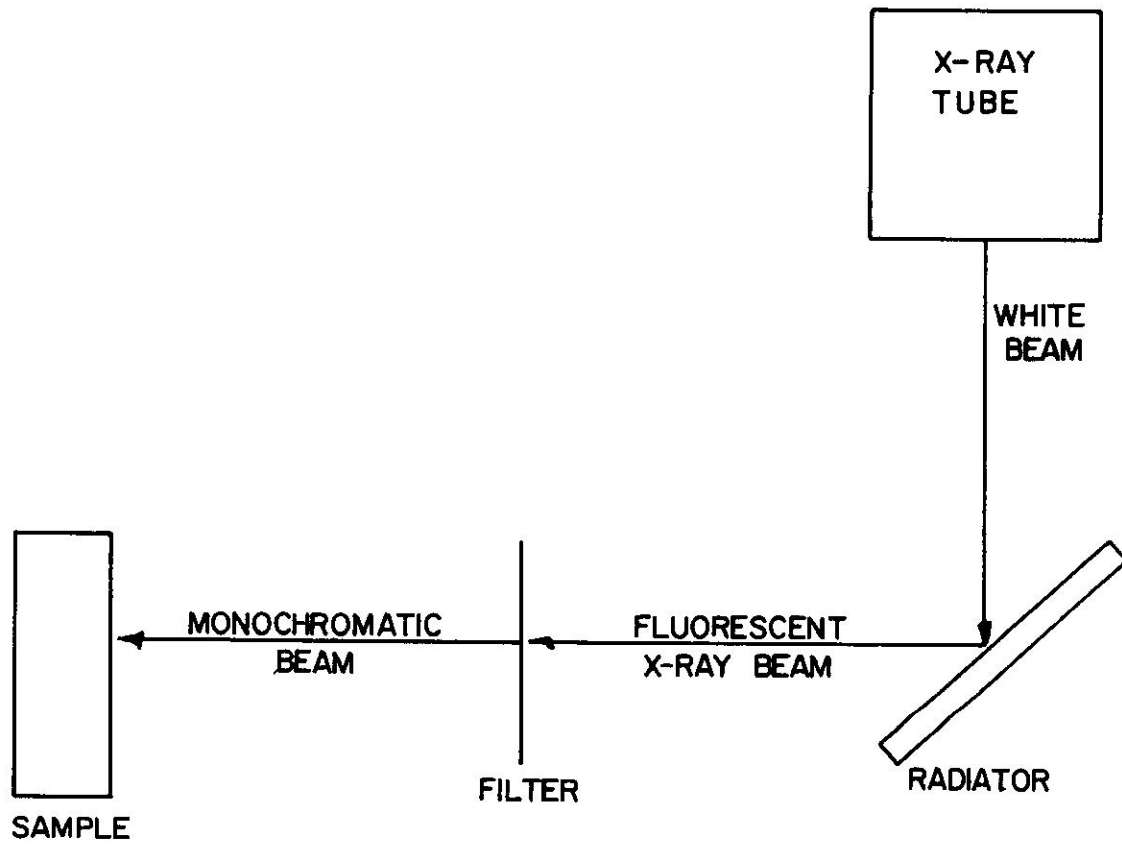
Figure 8.   Diagram of the production of monochromatic X rays
by the fluorescent technique.
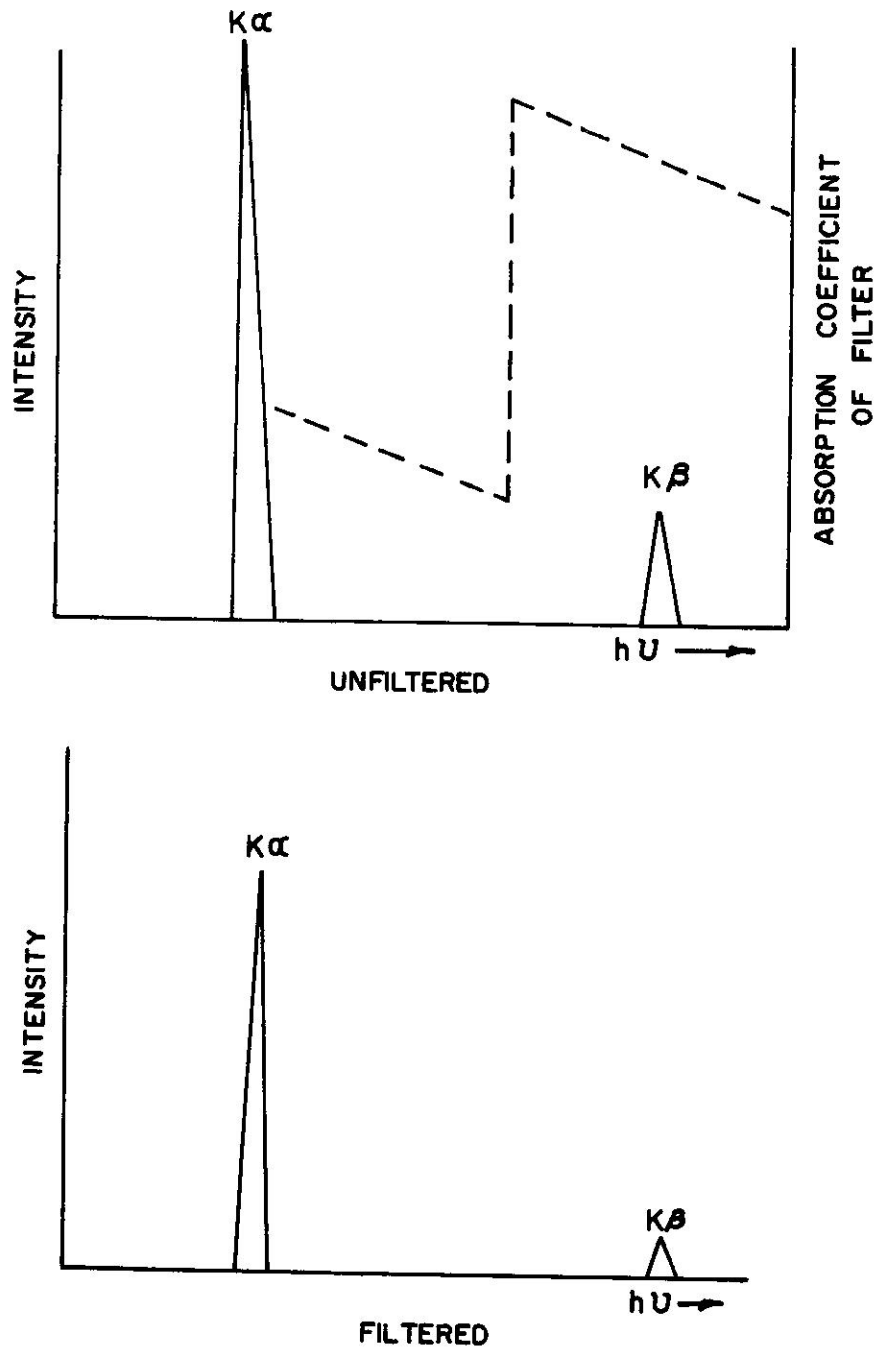
Figure 9. Filter action on the fluorescent output of the radiator. The dotted curve represents the absorption coefficient of the filter. After Gomberg, _et al_., reference 12.

The radiators and the filters which were used are listed in Table 1. See Figure 10. Two of the radiators, Se and Zr, were metallic. The other targets were made from fine powder that had been put through a 200 mesh sieve and then was tightly packed. The filters were prepared by suspending similarly sifted fine powder in a fresh solution of 50 percent Carter's 465 Cement and 50 percent acetone. The suspension was allowed to dry slowly on 1 mill mylar stretched over a plexiglass frame. Low humidity conditions were necessary to prevent the filter from blistering. The criteria for determining a good filter were that it appeared to be uniform and that it reduced the K_β peak to background level but did not reduce the K_α peak by more than 50 percent. The filters were tested by ordinary crystal diffraction techniques. The efficiencies of two of the filters are shown by the curves in Figures 11 and 12.

Photographic film which had been exposed at various distances in front of the window of the chamber that houses the radiator indicated that the beams were uniform in an area of about one square inch.

Likewise, the monochromaticity of the filtered fluorescent output was good. Tracings of the angular spectral analyses of the filtered output had a typical half-width of $2\theta \approx 0.4^\circ$, which corresponds to a spread in energy of approximately 330 eV. However, only energies

TABLE 1

RADIATORS AND FILTERS[a]

Radiator	Filter	Photon energy (keV)
Se metal	As_2O_3	11.2
NaBr powder	Se	11.9
RbCl powder	NaBr	13.4
$Sr(NO_3)_2$ powder	RbCl	14.1
$Y_2(CO_3)_3 \cdot 3H_2O$ powder	$Sr(NO_3)_2$	14.9
Zr metal	$Sr(NO_3)_2$	15.7

[a]The photon energy is that of the filtered output.
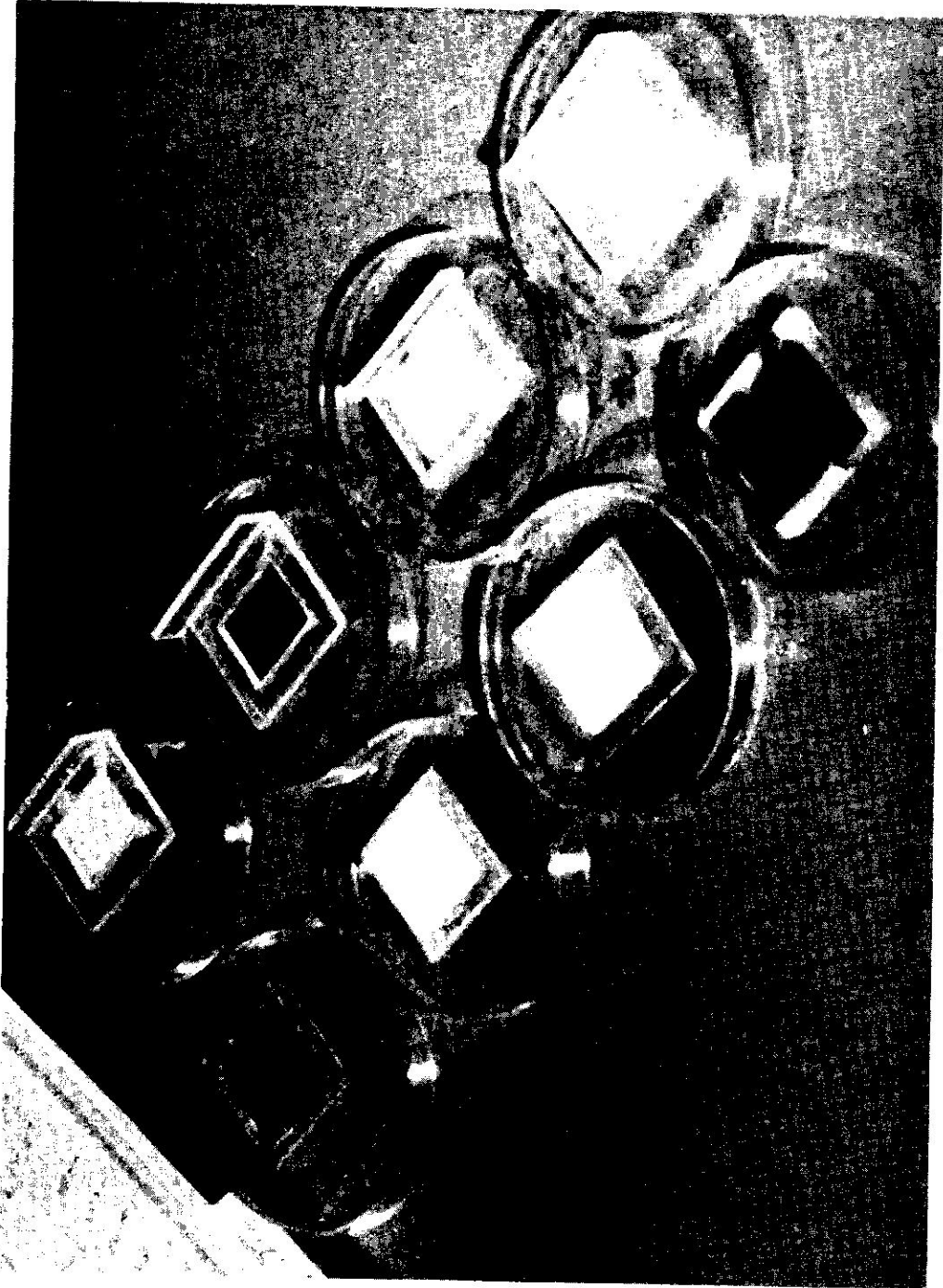
Figure 10. Some of the radiators and filters used in this work.
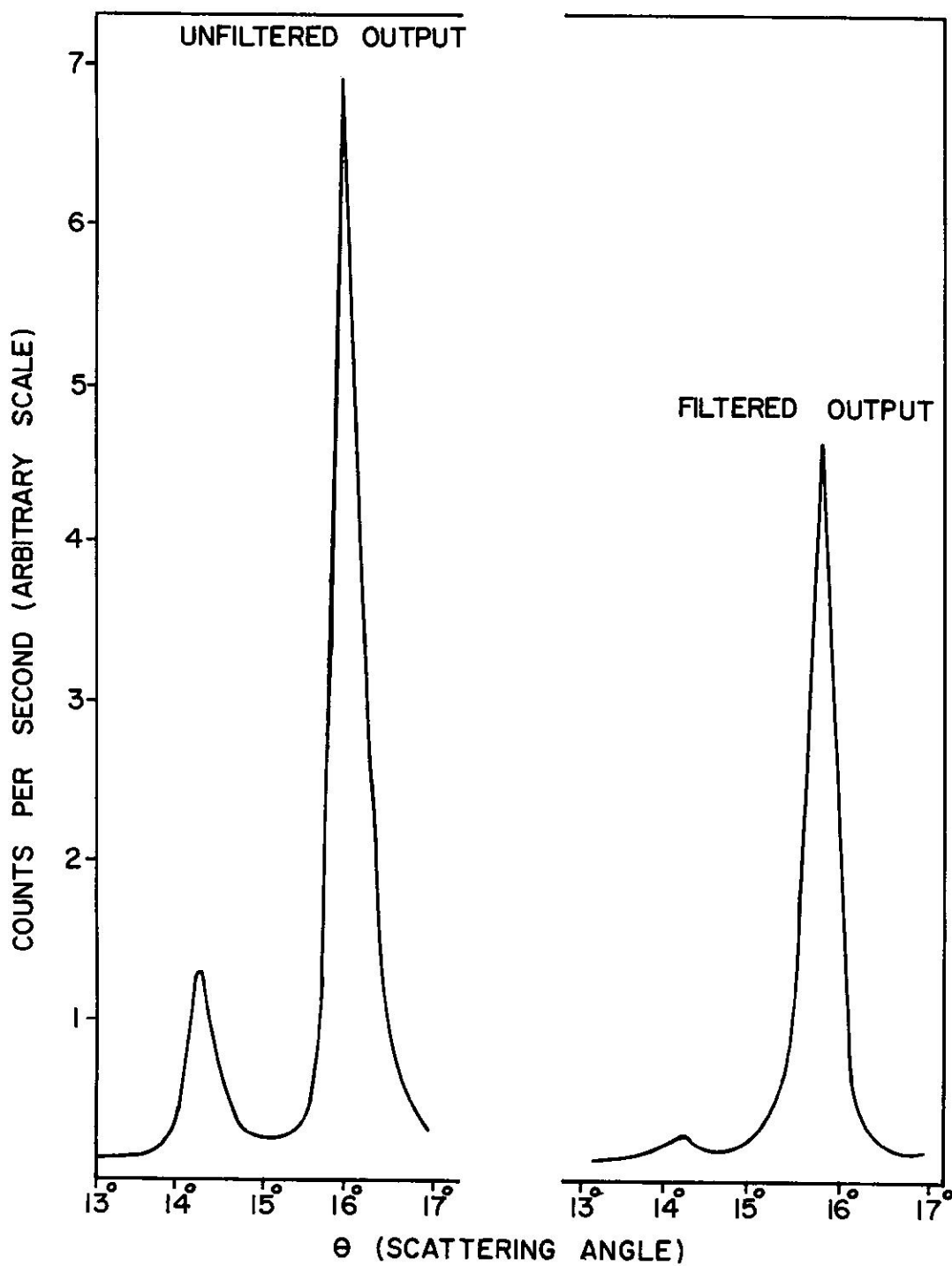
Figure 11. Spectrum analyses of the fluorescent emission of the RbCl radiator--before and after NaBr filtration.
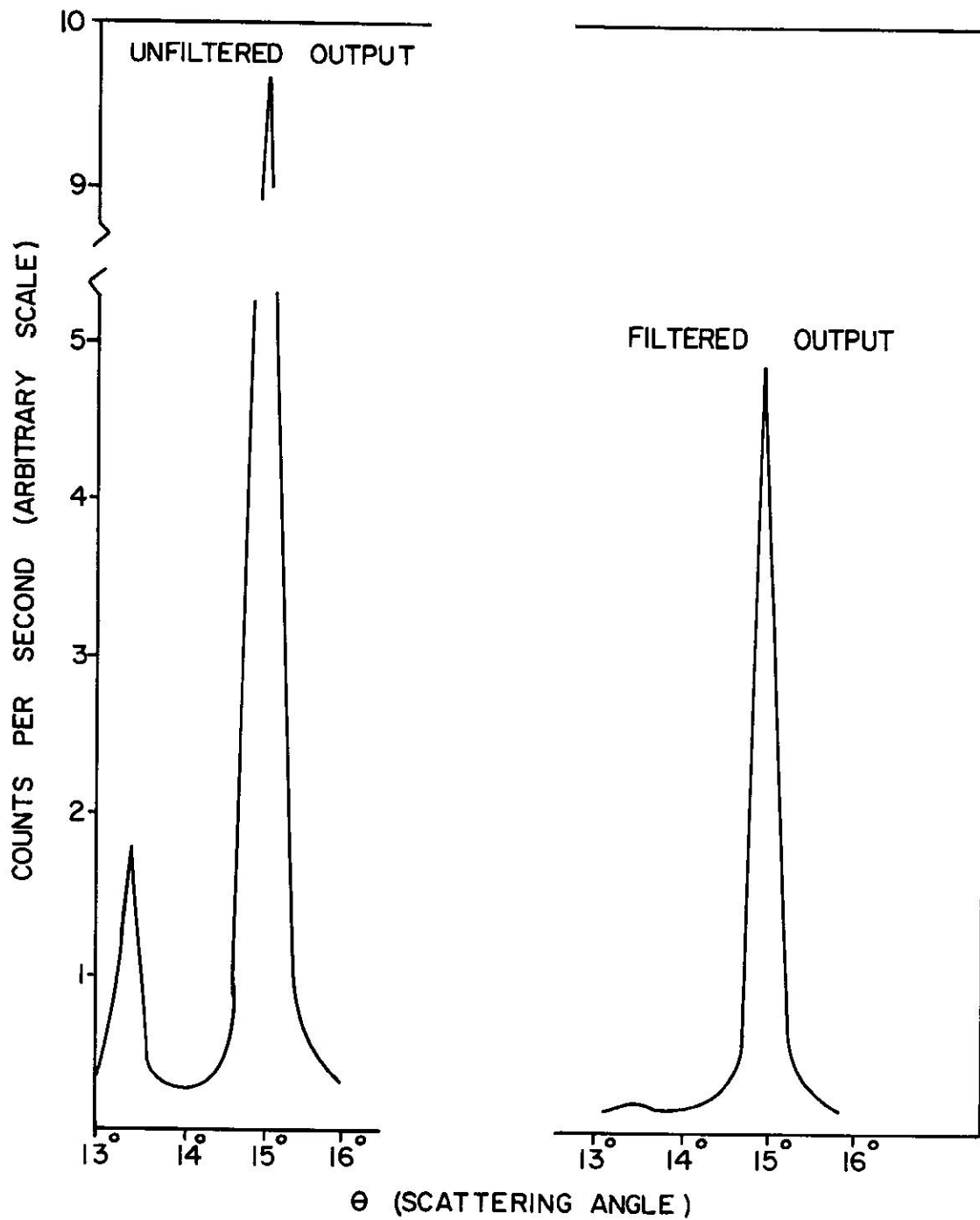
Figure 12. Spectrum analyses of the fluorescent emission of the $Sr(NO_3)_2$ radiator--before and after RbCl filtration. A quartz diffraction crystal was used.

arising from K_α emission lines were available. Thus, the absorption edge in the system to be studied could not be closely approached.

B. The Dosimeter

Further difficulty arose from the dosimetry. Ordinarily, the measurement of relative energy fluxes presents no major difficulty if the photon energies being used do not greatly differ from one another. In this experiment the problem was more difficult because the photon energies of one beam and another differed by several hundred volts. Likewise, the low ability of the radiation to penetrate made the energy flux measurements difficult. Actually, achieving accurate dosimetry was the most time-consuming problem in this work.

The first dosimetry system used in this work was the ferrous-ferric (Fricke) technique.[8] However, it proved to be inaccurate, probably because the intensity was too low and the irradiation periods were too long to prevent the influence of extraneous effects such as oxidation by exposure to light or evaporation of the solution.

Dosimetry runs in which silver activated phosphate glass was used were not reproducible to within 10 percent. Furthermore, the curve of optical density at a selected wavelength versus time of irradiation was not linear.

Also, good reproducible results can be expected only if the measurement of optical density is done several hours after irradiating. To follow this procedure was not convenient because a large number of measurements were required. Two NaCl crystal samples which were exposed in sequence to various energy fluxes also showed that the dosimetry based on short (30 minute) exposures of silver activated phosphate glass had a large random error.

After careful review of the problem of dosimetry, an air ionization chamber system was selected for use. The system consisted of an electrometer with a scale calibrated to read the total dose in roentgen units which was absorbed by a detachable charged condenser. It is manufactured by the Victoreen Instrument Company and consists of Model 570 Condenser R-Meter and Model 651 Air Ionization Chamber. This ionization chamber is intended for use in the range from 6 to 35 keV at a maximum rate of energy input of 90 roentgens per second. Figure 13 is a picture of the chamber in position for making X-ray intensity measurements.

Under low humidity conditions, readings consistently reproducible to within ±2 percent were obtained. A comparison of readings taken on different days shows a maximum variation of 5 percent, which is the manufacturer's rated accuracy for this instrument. In order to obtain the most consistent results possible, the ionization chamber

Figure 13. Victoreen Model 651 Air Ionization Chamber in position for dosimetry.

was discharged to the same extent in all cases. That is, the length of time it was exposed to the X-ray beams was varied to obtain approximately equal total roentgen exposure readings.

An advantage of the Victoreen dosimetry system was that a complete set of dosimetry measurements, for all radiators and at several values of the current in the primary X-ray tube, could be obtained in one day. Thus, it was possible to repeat the dosimetry and to verify the results several times.

Since the direct reading of the Victoreen Dosimeter is in roentgens, the reading must be divided by the time of exposure in order to obtain a measurement in roentgens per unit time. Since the roentgen is a unit of energy absorption and is dependent on the energy necessary to ionize the medium (air in this case), the change to absorbed energy values requires knowledge of the absorbed energy equivalent of one roentgen in air.

The energy equivalent of a roentgen in air is usually taken to be 86.9 ergs per gram of air. This corresponds to the assumption that 33.7 eV are needed to produce one ion pair in air.[110] However, when this value for the energy equivalent of a roentgen was applied to the experimental data or our, it gave a value for the energy of formation of one F center which was considerably larger

than previously reported values.[67] Thus, the energy equivalent of one roentgen (the term used to refer to one scale division of the Victoreen Model 570 Electrometer) has been determined by comparing readings of the dosimeter to direct energy flux measurements of a calorimeter. This calibration is discussed in Appendix A. Based on this calibration, the energy equivalent of one roentgen which was measured by the Victoreen Dosimeter in the range of photon energies from 13.4 to 15.7 keV is 11.3 ± .3 ergs per gram of air. When this value for the energy equivalent of one roentgen was applied to the experimental data on KBr, it gave a value for the energy of formation per F center which was in agreement with previously reported values.[67]

Absorbed energy values are converted to incident energy flux values by the following calculation. Let K be the absorbed energy equivalent of one roentgen in air in units of ergs per gram of air. Using centimeter-gram-second units, let ρ be the density and μ/ρ, the mass-absorption coefficient of air; V, the volume; d, the depth of the absorption cell; R, the absorbed dose in roentgens; t, the time of exposure; and F_i, the incident energy flux. In the geometry and the photon energy range which are used in this work: d is probably of the order of 1 cm; μ/ρ varies from 1.4 cm^2/gm to 3.8 cm^2/gm; and ρ is 1.29 x 10^{-3} gm/cc. Thus, the following relationships are valid:

$$1-e^{-(\mu/\rho)\rho d} \approx (\mu/\rho)\rho d, \text{ and}$$

$$\text{incident energy} \approx \frac{\text{absorbed energy}}{(\mu/\rho)\rho d}.$$

Then, the incident energy flux, F_i, in ergs/cm^2-sec is given by the relationships:

$$F_i = \frac{K\rho VR}{(\mu/\rho)\rho Vt} = \frac{KR}{(\mu/\rho)t} = \frac{(11.3)R}{(\mu/\rho)t}. \tag{1}$$

In every case that an energy flux (in ergs/cm^2-sec) is reported, the value has been obtained by application of Equation (1) to the readings of the dosimeter and of the timer.

C. The Calorimeter

Two factors made the use of a calorimeter desirable: First, the photon energies which were used in the experiment were in an energy range in which the mass-absorption coefficient of air changes. This change affected the accuracy of the energy flux measurements which were obtained from the roentgen exposure readings of the Victoreen Dosimeter. Therefore, in order to obtain an absolute measurement of the efficiency of formation of F centers, absolute incident energy flux measurements had to be made.

Second, to be able to refer the measurements to an absolute standard is an advantage because any other researcher will be able to duplicate the conditions of the experiment.

The calorimeter which was used had been designed and built at the University of Michigan.[6] See Figures 14, 15, and 16. The calorimeter operates at liquid nitrogen temperature. The incident X-ray flux is admitted to the calorimeter vessel through an aluminized mylar window and a cold beryllium window, and then it is absorbed by a cold but electrically and thermally insulated gold target. The gold target is designed to be totally absorbent in the energy range of the experiment. It consists of two layers of gold foil and a coiled heater wire of known resistance located between the foil layers. Two thermistors are thermally connected to the back of the target. These thermistors form two resistances of a Wheatstone bridge, which gives a signal indicating change in temperature when an X-ray beam is incident on the target. To calibrate the instrument the signal which is generated by the heater coil of the gold target is recorded when a known current is supplied. The instrument was calibrated in a range corresponding to an energy absorption of less than 100 nanowatts. A program of absolute calibration of the calorimeter plus calibration of several dosimetry systems is being conducted by

P. Paraskevoudakis and three students who have been working
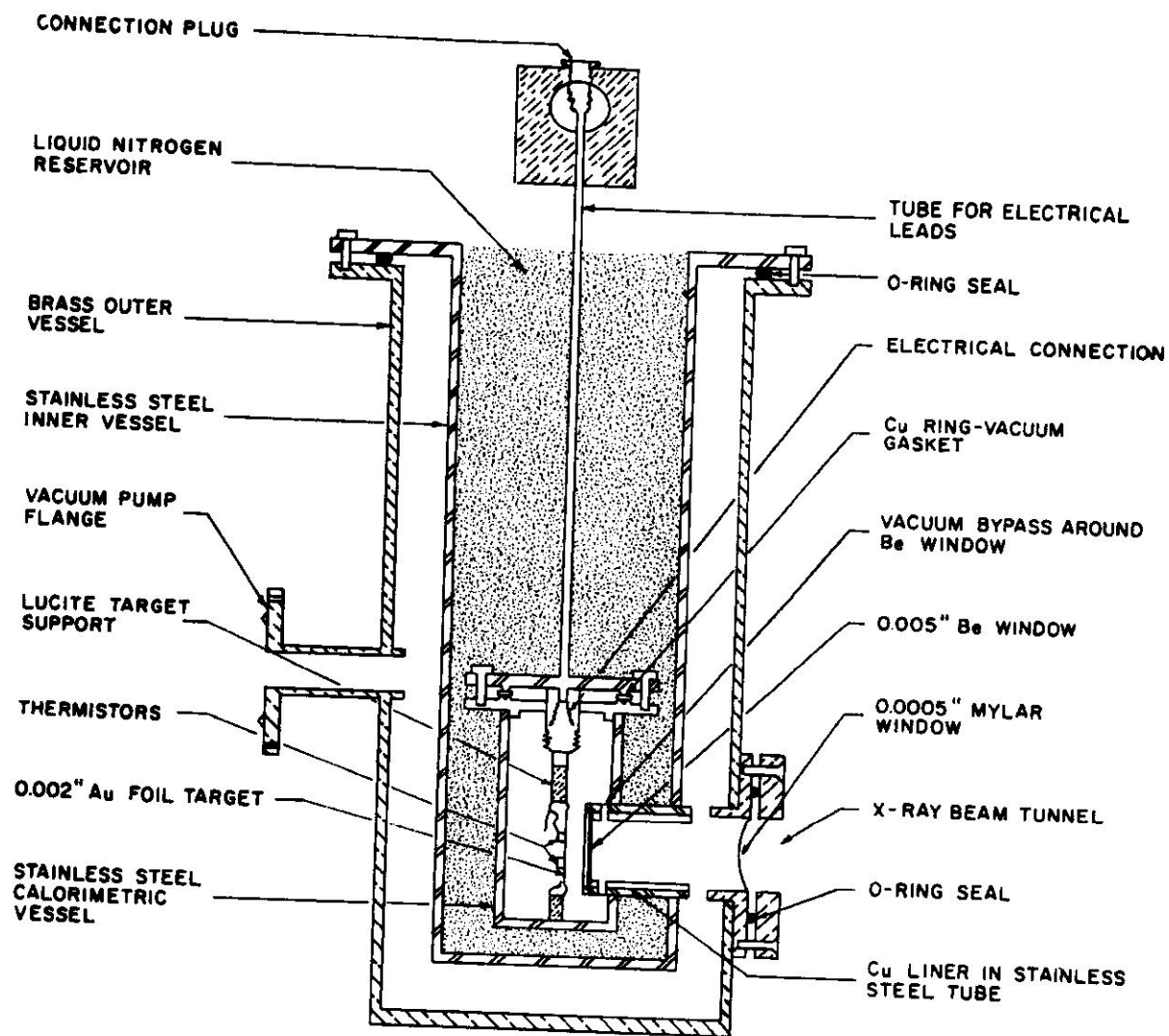
Figure 14. Diagram of the X-ray calorimeter used in this work. After Gomberg, *et al*., reference 10.
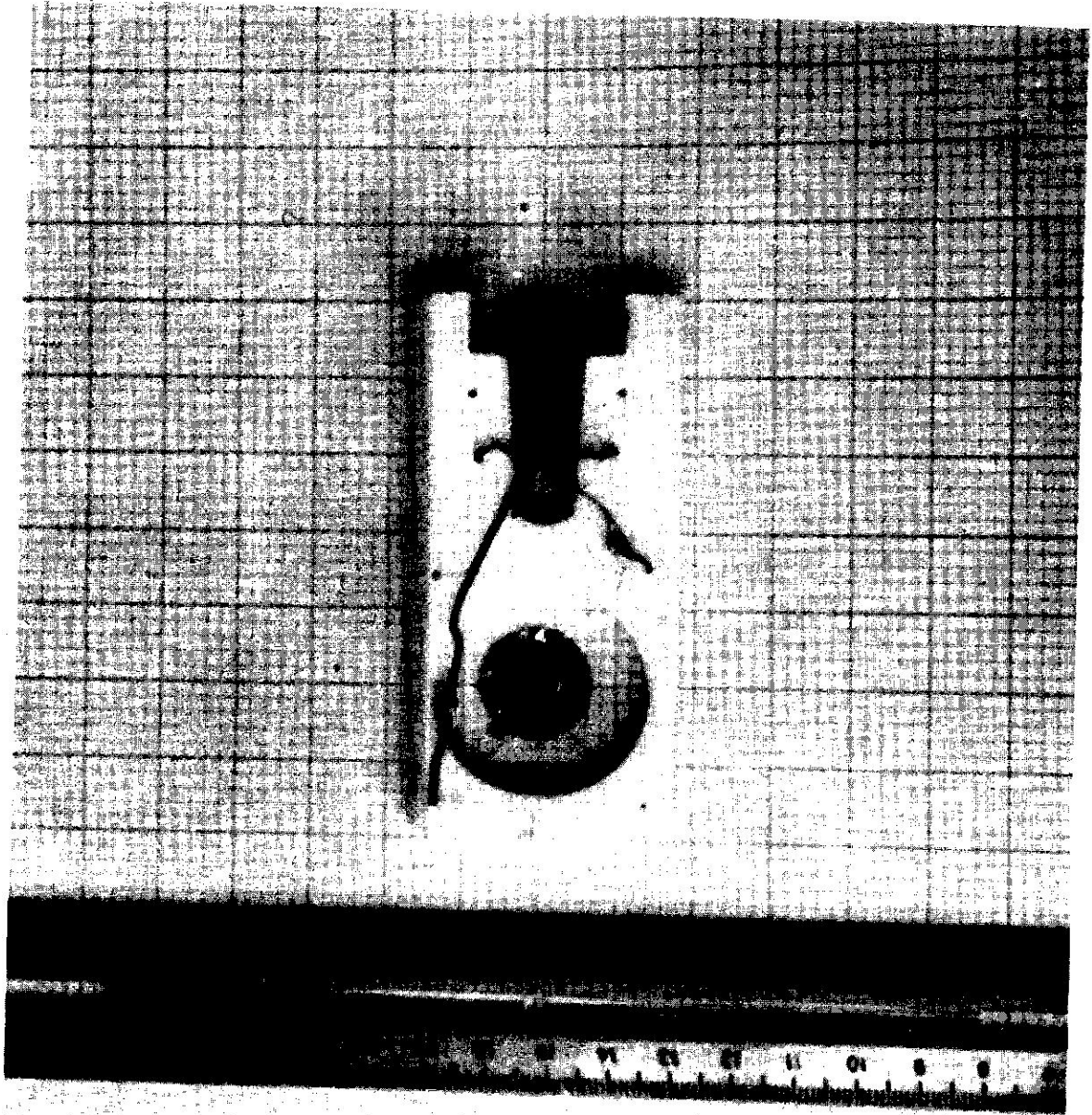
Figure 15.   The gold target of the X-ray calorimeter.
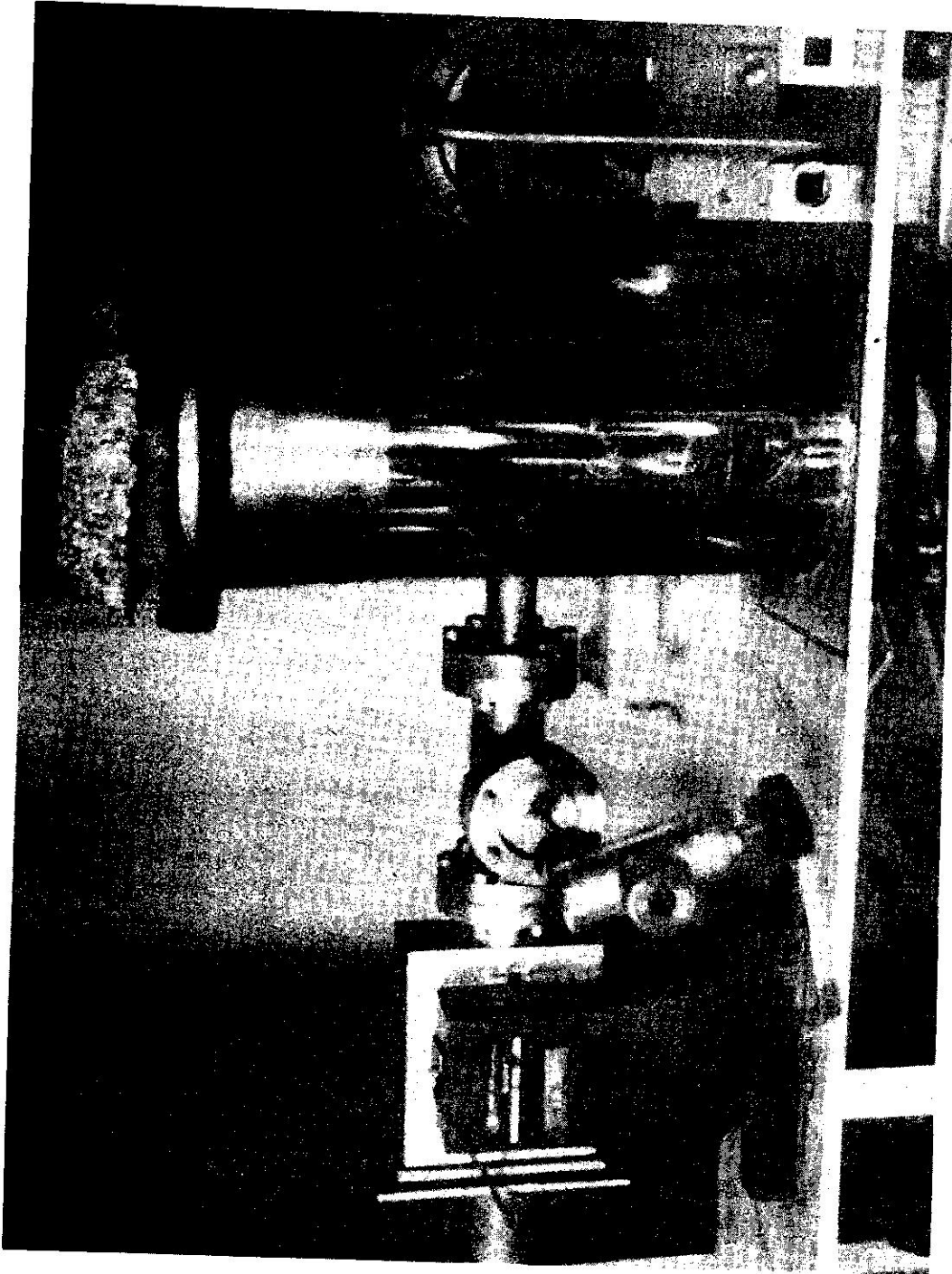
Figure 16. The X-ray calorimeter in position on the X-ray unit.

for their Master's degrees in Nuclear Engineering. As part of that program, calibration runs have been made on the Victoreen system. These runs are reported in Appendix A.[111,112]

D. Other Equipment

1. The spectrophotometer

Throughout the work a Beckman DU Spectrophotometer was used. See Figure 17. It is rated by the manufacturer as being capable of transmissivity measurements in the range from 2000 to 20,000 Angstroms (200 to 2000 millimicrons).

For the runs at liquid nitrogen temperature a sample box capable of enclosing the bottom of the low temperature dewar was constructed. The spread in the light beam of the spectrophotometer necessitated the use of a focusing lens. Even when using quartz optics exclusively, the optical losses were too high and the ultraviolet sensitivity of the instrument was too low to make measurements of the α band in KBr possible. Thus, unfortunately, that band has not been studied. Similarly, since the X-ray intensities used in this work are low by comparison to the intensity obtainable with the direct full output of an X-ray tube, the V bands produced were too weak to be measured quantitatively.
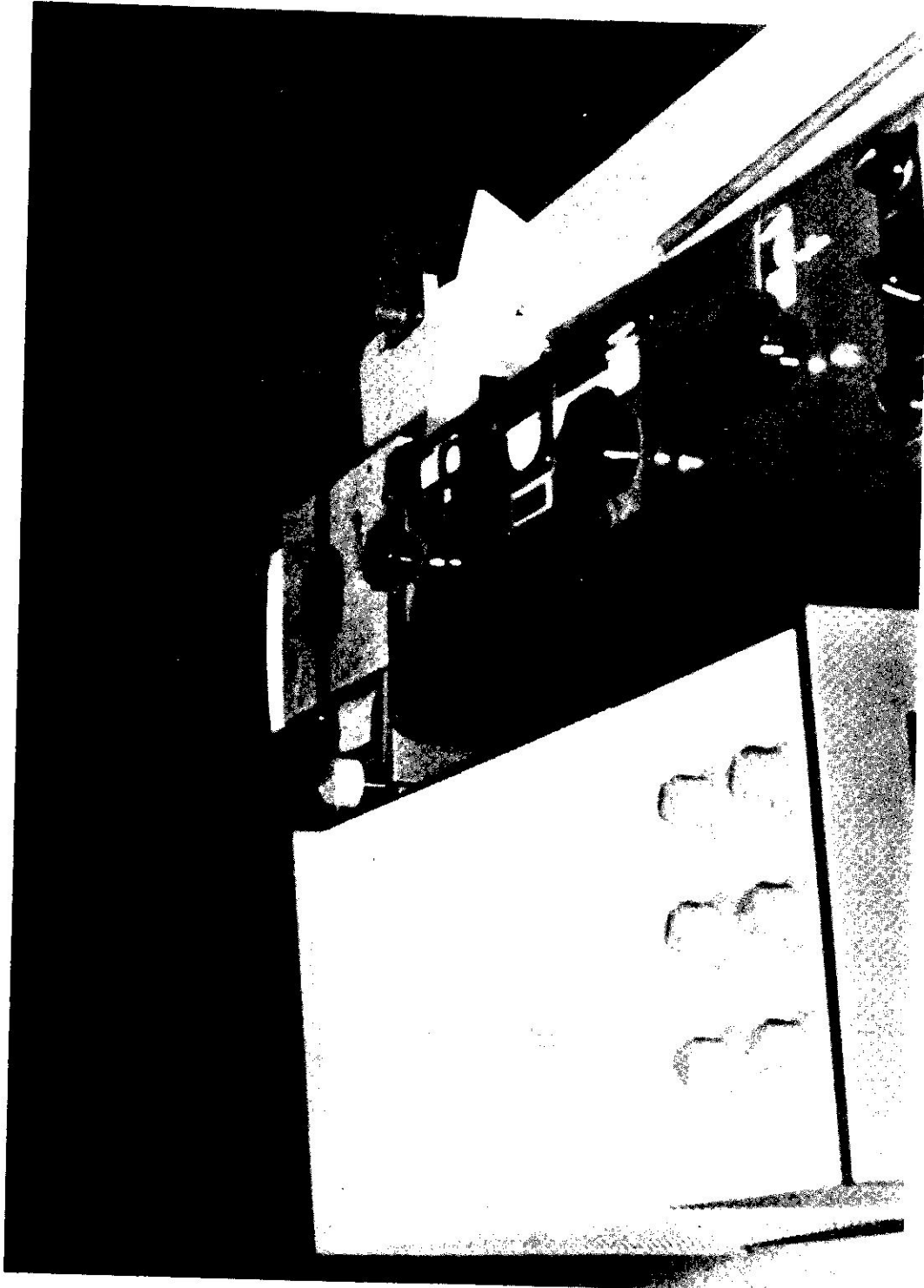
Figure 17. The Beckman DU Spectrophotometer.

2. The low temperature dewar

Throughout the work a liquid helium dewar manufactured by Superior Air Products Company was used. See Figure 18. The irradiation window consisted of a tightly stretched mylar film 0.001 inch thick. Opposite this window a quartz (or a thick mylar) window was mounted. The optical absorption of the crystal was measured through the two windows.

The sample was mounted on a copper rod which was at liquid nitrogen temperature. Through the middle of that copper rod two parallel holes, each approximately 3/8 inch in diameter, had been drilled 1/2 inch apart. On one hole the sample was glued with either low vapor pressure epoxy or vacuum grease. The other hole was left unobstructed to serve as the reference in the transmissivity measurements.

When mounted on the sample holder of the Beckman Spectrophotometer, the dewar rested on rails on which it could slide in order to place either the unobstructed hole or the sample in the path of the light beam.

E. Sources of Crystals

RbBr crystals which were used in this work were cleaved from a larger crystal that had been purchased from the Isomet Corporation. The crystals were of poor physical
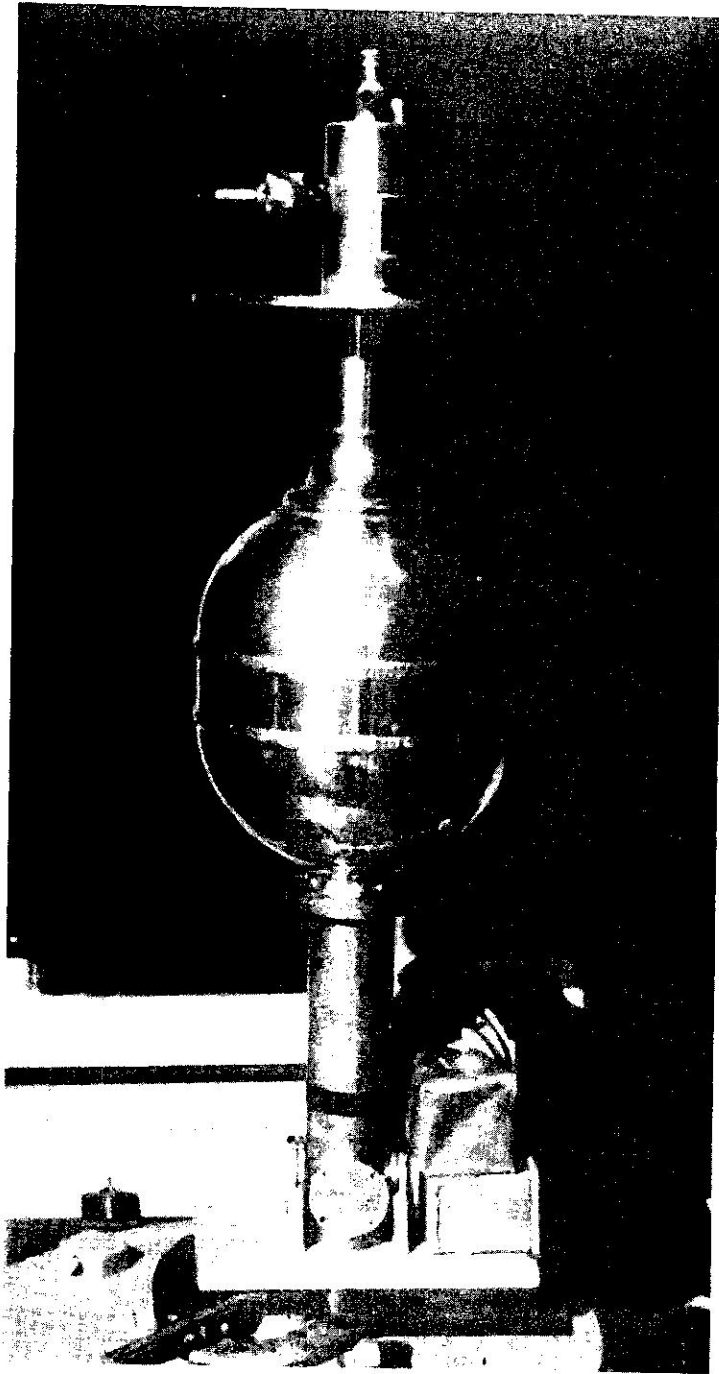
Figure 18. The low temperature dewar
mounted on the X-ray unit.

quality, readily seen with the unaided eye.

Crystals of KBr, of NaCl, and of KCl which were studied were cleaved from larger blocks which had been purchased from the Harshaw Chemical Company. All these crystals appeared to be of good physical quality. No tests, however, were made of their chemical purity.

F. Smakula's Equation

Smakula's equation was used to quantitatively evaluate the radiation damage. The equation relates the absorption coefficient at the maximum of the F band to the density of F centers in the crystal. It was first derived by A. Smakula, who applied classical dispersion theory to a damped oscillator model of the F center.[113] He obtained the following equation:

$$Nf = \left[\frac{9n}{(n^2 + 2)^2}\right]\left[\frac{mc}{\pi e^2}\right]\left[\frac{\pi}{2}\alpha W\right] = 1.29 \times 10^{17}\left[\frac{n}{(n^2 + 2)^2}\right]\alpha W \, ,$$

where: $\left[\frac{\pi}{2}\alpha W\right]$ is the area under the F absorption curve whose shape is assumed to be Lorentzian; N is the number of F centers per cubic centimeter; f is the oscillator strength, which can be considered to be an experimentally determined constant[114]; n is the index of refraction at the peak of the F band; W is the half-width of the F band, measured in

electron volts; and α is the absorption coefficient, measured in $(centimeters)^{-1}$, at the peak of the F band.

The following relationship is valid:

$$\alpha = \frac{1}{d} \frac{A}{\log_{10}e} = \frac{1}{0.434d} \log_{10}\left[\frac{I_o}{I_T}\right],$$

where: $A = \log_{10}\left[\frac{I_o}{I_T}\right]$ is the absorbance at the peak of the F band and is measured directly by the spectrophotometer; d is the thickness of the crystal in centimeters; I_o is the incident intensity; and I_T is the transmitted intensity at the maximum of the F band.

Therefore, Smakula's equation can be expressed as

$$Nd = 1.19 \times 10^{16}A \text{ for KBr and for RbBr at } 300^{\circ}K \qquad (2)$$

and as

$$Nd = 5.57 \times 10^{15}A \text{ for KBr and for RbBr at } 78^{\circ}K. \qquad (3)$$

In the above calculation the following values were used: $W = 0.41$ eV for RbBr and for KBr at $300^{\circ}K$; $W = 0.19$ eV for RbBr and for KBr at $78^{\circ}K$; and $f = 0.80$ for RbBr and for KBr. The values given for W were verified experimentally and were found to agree with the indicated values which had been reported.[115] The value given for f is within the range of

experimentally determined values.[116]

G. Experimental Procedure

Several crystals of KBr were irradiated. The usual procedure was to alternate a period of irradiation which lasted 6 to 12 hours with a short period of observation of the absorbance in the region of the F and the F', and the V bands.

Five of the runs at liquid nitrogen temperature (78°K) were done on KBr crystals where each crystal was exposed only to 13.4 keV photons or only to 14.1 keV photons. The runs usually were 60 hours long. In every run the current setting of the X-ray tube was adjusted to achieve equal energy flux on the face of the crystal. During the optical measurements, a maximum of 2 percent of the F centers was bleached. But, when extensive measurements were done in the region of the F' band, growth of the F band was observed.

Several other runs were done on KBr crystals at 78°K. During each of these runs several incident photon energies were used in random sequence. Absorbance measurements were made between changes of the incident photon energy. The results of this work are expressed as rates of F center formation per unit incident energy, $\frac{dF}{dE_i}$, or absorbed energy, $\frac{dF}{dE_a}$, as a function of incident photon energy. These

runs, where the photon energy was changed, gave only short line segments for the computation of these rates. Thus, these rates have a larger error than the rates which were computed from the curves which had been obtained by exposure to only one photon energy. Nevertheless, all of the growth curves which had been obtained gave results which are qualitatively consistent with the conclusions of this work.

Several samples of KBr were irradiated at room temperature (300°K). Since the coloration is slow at 300°K, an individual run required as much as 200 hours. Each sample was exposed to several photon energies. During an optical measurement as much as 5 percent of the F center concentration was bleached. Because of this bleaching, the measurements which were obtained at room temperature had a larger error than those which were obtained at liquid nitrogen temperature. Thus, primary consideration has been given to the results at liquid nitrogen temperature. The data at room temperature has been reported only in Appendix B and was used to calculate the energy of formation of one F center while disregarding incident photon energy.

One crystal of RbBr was exposed to X rays under the same conditions as those described above for the room temperature irradiation. During the short time it took to make one optical measurement, between 30 and 50 percent of the F center concentration was bleached. Thus, no further

attempt was made to obtain data on RbBr at room temperature.

One RbBr sample was exposed at 78°K to different photon energies but to equal energy flux. During each optical absorption measurement up to 10 percent of the F centers was bleached. Thus, further experimentation on RbBr would have been of limited value. However, the run did indicate, by a decrease in the slope of the growth curve, that as the photon energy becomes greater than an absorption edge, some incident energy is lost by fluorescence.

One NaCl crystal was irradiated at 300°K. This run was done in order to check the dosimetry readings which had been based on the silver activated phosphate glass, and to check the preliminary readings based on the Victoreen Dosimeter.

Late in the experimental program one KCl sample was exposed at 78°K to various photon energies but to the same energy flux. The growth curve remained smooth as the photon energy was changed. Also, no bleaching of F centers was observed, so the optical measurements on this crystal are considered to be particularly good. Thus, this run was valuable because it helped to verify that the X-ray tube current whose value was dictated by the Victoreen Dosimeter achieved equal energy fluxes on the sample regardless of incident photon energy. This run has been included in Appendix B.

H. Experimental Results

1. The rate of F center formation per unit incident energy on KBr at 78°K

Figure 19 shows the growth curves of coloration at the peak of the F band for KBr crystals which were each exposed at 78°K to monochromatic X-ray photons of either 13.4 keV or 14.1 keV. The plot shows the absorbance versus the time of exposure to X rays. The lines on the figures are the least square straight lines which best fit the experimental points in the region of the growth curve that seems to be linear. The experimental points for each run in the linear-growth region are tabulated in Table 2. The slope of the least square curve fitted to each set of experimental points is given in the table.

Using Smakula's equation the rate of F center formation per square centimeter in KBr at 78°K was derived:

$$\frac{d(Nd)}{dt} = 5.57 \times 10^{15} \frac{dA}{dt} . \qquad (4)$$

By dividing $\frac{d(Nd)}{dt}$ by the incident energy flux, F_i (given in units of energy per square centimeter per unit time), the rate of growth of F centers per unit incident energy, $\frac{dF}{dE_i}$, was obtained. Thus, for KBr at 78°K, $\frac{dF}{dE_i}$ is given by the

68
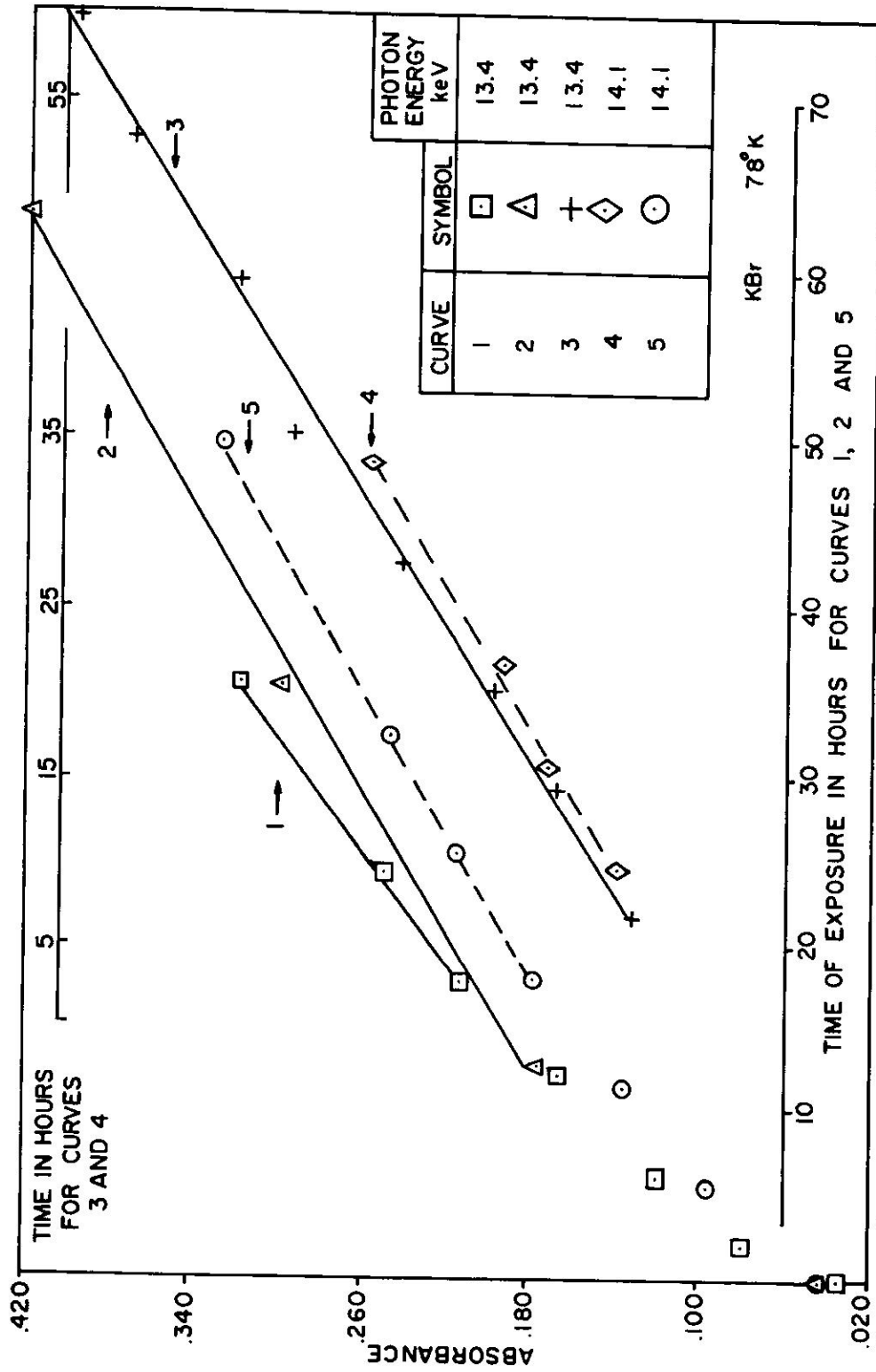
Figure 19. Absorbance at the peak of the F band of KBr irradiated at 78°K--plotted as a function of exposure time. For each run the incident photon energy is given in the inset. All runs were made at the same energy flux. For each run the straight line is the least square fit to the experimental points through which the line is drawn.

TABLE 2

EXPERIMENTAL POINTS CORRESPONDING TO THE CURVES IN FIGURE 19[a]

Curve	Time (hours)	Absorbance	Slope of least square straight line (hours^{-1})	Average of corrected slopes (hours^{-1})	Standard deviation of the average
1	17.8 24.1 35.3	0.214 0.250 0.319	0.00602		
2	13.6 35.55 62.95	0.180 0.298 0.420	0.00485		
3	6.8 14.4 20.1 27.7 35.2 44.2 52.52 59.8	0.133 0.170 0.197 0.242 0.293 0.321 0.370 0.397	0.00509	0.00532	± 0.00034
4	9.5 15.5 21.5 33.5	0.140 0.173 0.195 0.258	0.00480[b]		
5	17.8 25.6 32.3 49.6	0.177 0.216 0.248 0.328	0.00473	0.00477	± 0.00004

[a]Curves 1, 2, and 3 were obtained at an incident photon energy of 13.4 keV; curves 4 and 5 were obtained at 14.1 keV.

[b]A correction of 1 percent has been subtracted from the value of the slope of curve 4 to correct for the fact that during the run the tube current was 1 percent higher than it should have been.

following equation:

$$\frac{dF}{dE_i} = \frac{5.57 \times 10^{15}}{F_i} \frac{dA}{dt} \,.$$

For all the experiments which were done in the preparation of this thesis, the incident energy flux was:

$$F_i = 5.77 \times 10^4 \; (\pm \; 2\%) \; ergs/cm^2\text{-hr.}$$

This value for F_i was obtained by substituting the experimentally determined value of $\frac{R}{(\mu/\rho)t} = 1.46 \; (\pm \; 2\%)$ roentgen-gm/cm^2-sec in Equation (1).

Thus, for the experiment on KBr at 78°K the efficiency of formation of F centers in units of F centers formed per erg is

$$\frac{dF}{dE_i} = 0.966 \times 10^{11} \frac{dA}{dt} \; (\pm \; 3.6\%) \; ergs^{-1},$$

where $\frac{dA}{dt}$ is in units of (hours)$^{-1}$. The same efficiency of formation of F centers, but in units of F centers formed per electron volt is

$$\frac{dF}{dE_i} = 0.154 \frac{dA}{dt} \; (\pm \; 3.6\%) \; ev^{-1}, \tag{5}$$

where $\frac{dA}{dt}$ is in units of (hours)$^{-1}$.

The uncertainty stated in the last two equations was computed from the following two errors: first, a 3 percent uncertainty in the change of absorbance (ΔA); and second, a 2 percent uncertainty in the statement that the energy flux is the same in the runs in which 13.4 keV photons were used as in the runs in which 14.1 keV photons were used.

Since the energy flux was the same in the runs in which 13.4 keV photons were used as in the runs in which 14.1 keV photons were used, the constant of proportionality in Equation (5) is the same for both photon energies.

The rate of growth of absorbance per hour of exposure to X rays, $\frac{dA}{dt}$, is larger in the runs in which 13.4 keV photons were used than in the runs in which 14.1 keV photons were used. The experimental data are presented in Table 2. Also, since the constant of proportionality in Equation (5) does not change when the incident photon energy changes, the rate of F center formation per unit incident energy, $\frac{dF}{dE_i}$, is larger in the runs in which 13.4 keV photons were used than in the runs in which 14.1 keV photons were used. These results can be expressed by the following equations:

$$\frac{\left[\dfrac{dA}{dt}\right]_{13.4\ keV}}{\left[\dfrac{dA}{dt}\right]_{14.1\ keV}} = \frac{53 \pm 3.4}{48 \pm 1.7} \ ,$$

$$\frac{\left[\dfrac{dF}{dE_i}\right]_{13.4\ keV}}{\left[\dfrac{dF}{dE_i}\right]_{14.1\ keV}} = \frac{53 \pm 3.4}{48 \pm 1.7} \ . \tag{6}$$

In the last two equations the error given for the slope at 13.4 keV is the standard error of the average of the slopes of curves 1, 2, and 3 in Figure 19. This error, as well as the error for the slope at 14.1 keV, is discussed in Section III-H-5.

2. Correction due to K shell fluorescence

When the incident photon energy is above the energy of the K absorption edge of a sample, a fraction of the incident energy is emitted as fluorescence. Thus, in order to obtain the efficiency of formation of F centers per unit absorbed energy in KBr, a correction for fluorescence must be made whenever the incident photon energy is above the energy of the bromine K absorption edge.

The calculation of fluorescent loss by W. J. Veigele and N. J. Roper[117] was followed in the derivation of the correction to be applied to the efficiency of formation of F centers per unit incident energy in KBr when the incident photon energy is 14.1 keV (where the energy of the K absorption edge of bromine is 13.5 keV). The derivation is given in Appendix C. The result follows: When 14.1 keV photons are incident on a KBr crystal slab, 10.2 percent of the incident energy is lost in the form of fluorescence from the face of the crystal exposed to the photon beam. The fluorescence through the back face of the crystal is negligible. When the photon energy is below the energy of the K absorption edge, no fluorescent loss results.

3. The rate of formation of
F centers per unit absorbed
energy in KBr at 78°K

The calculation in Appendix C showed that when the incident photon energy on KBr is 14.1 keV, which is larger than the energy (13.5 keV) of the K absorption edge of bromine, 10.2 percent of the incident energy flux was lost by fluorescence through the front face of the crystal. Accordingly, an expression for the efficiency of formation of F centers per unit absorbed energy in the crystal, $\frac{dF}{dE_a}$, has been derived. This expression shows that when 13.4 keV photons (below the bromine K absorption energy) are incident

on KBr, essentially all the incident energy is retained in the crystal. However, when 14.1 keV photons (above the bromine K absorption energy) are incident on KBr, only 89.8 percent of the incident energy is retained in the crystal. This result is stated in the following equations:

$$\left[\frac{dF}{dE_a}\right]_{13.4\ keV} = \left[\frac{dF}{dE_i}\right]_{13.4\ keV} , \text{ and}$$

$$\left[\frac{dF}{dE_a}\right]_{14.1\ keV} = \frac{1}{0.898}\left[\frac{dF}{dE_i}\right]_{14.1\ keV} .$$

Using the last two equations and Equation (6), the following result has been derived:

$$\frac{\left[\frac{dF}{dE_a}\right]_{13.4\ keV}}{\left[\frac{dF}{dE_a}\right]_{14.1\ keV}} = \frac{53 \pm 3.4}{53 \pm 1.9} . \tag{7}$$

According to the last equation, within the uncertainty of the result, the rate of formation of F centers per unit absorbed energy in KBr is the same whether the ionizing radiation consists of 13.4 keV photons

or 14.1 keV photons. Therefore, the energy which is required to form an F center (the inverse of $\frac{dF}{dE_a}$) is the same for the two incident photon energies.

Table 3 summarizes the results already presented in this thesis. The errors shown in the table and in the last equation are the standard errors derived for the purpose of comparing the rates of formation at the two incident photon energies. Further contributions to the error in each rate of formation or in each energy of formation originated from the uncertainty in the calorimetric calibration of the dosimetry and from errors introduced with the constants in Smakula's equation.

4. The energy of formation of one F center in each of several alkali halides

During the experimental study of the role of the bromine K ionization in the formation of F centers in KBr, other alkali halides were irradiated with the monochromatic X-ray beams. For each of the alkali halides the energy of formation of one F center at the given temperature of exposure was computed when the calorimetric calibration of the beams became available. These computed values are listed in Table 4. The growth curves of coloration from which these values of the energies of formation were computed are in Appendix B. In all cases the curves were

TABLE 3

THE EFFICIENCY OF FORMATION OF F CENTERS AND THE ENERGY OF FORMATION OF ONE F CENTER IN KBr AT 78°K DURING EXPOSURE TO MONOCHROMATIC X RAYS

Incident photon energy (keV)	Efficiency of formation of F centers: per incident energy, $\frac{dF}{dE_i}$ (eV^{-1})[a]	per absorbed energy, $\frac{dF}{dE_a}$ (eV^{-1})[a]	Energy of formation of one F center, E_F (eV)[b]
13.4	$8.25 \times 10^{-4} \pm 6.4\%$	$8.25 \times 10^{-4} \pm 6.4\%$	$12.1 \times 10^2 \pm 4.9\%$
14.1	$7.25 \times 10^{-4} \pm 3.6\%$	$8.25 \times 10^{-4} \pm 3.6\%$	

[a]The uncertainties in dF/dE_i and in dF/dE_a are described in Section III-H-5.

[b]The uncertainty in E_F is the standard error of the average value of E_F computed from the data in Figure 19. The standard deviation (3.5%) of the average value of the slopes of all curves in Figure 19, the uncertainty (2%) in the dosimetry, and the uncertainty (2.7%) in the calorimetry were considered.

TABLE 4

ENERGY OF FORMATION (E_F) OF ONE F CENTER IN
SOME ALKALI HALIDES DURING EXPOSURE TO
MONOCHROMATIC X RAYS
AT 78°K AND 300°K

Alkali halide	E_F at 78°K (eV per F center)	E_F at 300°K (eV per F center)
KCl	$6.9 \times 10^2 \pm 4.2\%$[a,b]	not measured
KBr	$1.21 \times 10^3 \pm 4.4\%$[a]	$4.8 \times 10^3 \pm 5.7\%$[a,c]
RbBr	$1.2 \times 10^3 \pm 17\%$[d]	$1.3 \times 10^3 \pm 30\%$[e]

[a]The slope of the growth curve of coloration, the dosimetry, and the calorimetry have each contributed an uncertainty to this result.

[b]A correction of 2% for the energy transmitted through the sample was included in this result. (See Figure 25 of Appendix B.) No correction for fluorescent loss was included in this result.

[c]A correction of 9% for fluorescent loss was included in this result. (See Figure 24 of Appendix B and Table 11 of Appendix C.)

[d]The uncertainty is the standard deviation of the average of the slopes of the growth curves of F band coloration. (See Figure 26 of Appendix B.)

[e]The uncertainty is due to the bleaching of the F band during the optical measurements. (See Figure 27 of Appendix B.)

obtained by exposing the irradiated crystals to one or more
of the following photon energies: 11.2 keV, 11.9 keV,
13.4 keV, 14.1 keV, 14.9 keV, and 15.7 keV.

5. Discussion of the experimental errors

The only error affecting the rate of growth of the
absorbance per unit time of exposure to X rays is the
variation of the absorbance during the optical measurements.
For KBr at 78°K the variation was small--usually, 2 to
3 percent of the value of the absorbance but, in a few
cases, as high as 6 percent. Since the rates of growth of
absorbance are the slopes of curves, drawn through several
experimental points, each error was estimated from the
standard error of a value obtained by using a least square
fit to the experimental points.

Let A_1, A_2, $\cdots$, A_n be the n measured values of the
absorbance at the respective times t_1, t_2, $\cdots$, t_n. If a
straight line is fit through these points, then at any
time t the value A estimated from the fitted curve will have
a standard error equal to the sum of the square of the
deviations of the fitted curve from the experimental points
divided by n. If one assumes that the time measurements
(Δt) have a negligible error, then the percent error of the
slope, $\frac{dA}{dt}$, would be the same as the percent error of the
change in absorbance (ΔA). Therefore, assuming that the

slope is computed by subtracting estimated values at both ends of the range t_1 to t_n, the percent error of the slope would be given by the relationship:

$$\text{percent error of the slope} = \frac{2(\text{standard deviation})}{(A_n - A_1)} \times 100$$

The percent error of the slope for each of the curves in Figure 19 was calculated and is shown in Table 5.

The standard error of the average value of the slopes for the three curves at 13.4 keV is 6.4 percent, shown in Table 6.

An examination of the errors of the two curves at 14.1 keV indicates that at this photon energy a standard error of 2.9 percent may be assumed. See Table 5.

Since the energy fluxes were the same regardless of incident photon energy, a comparison of the slopes, $\frac{dA}{dt}$, as a function of photon energy is equivalent to a comparison of the rate of formation of F centers per unit incident energy, $\frac{dF}{dE_i}$, as a function of photon energy. Any variation between the incident energy fluxes at the two photon energies was caused only by uncertainties in the dosimetry readings and in the values used for the mass absorption coefficient of air. Under low humidity conditions the dosimetry readings gave results whose uncertainty was not

TABLE 5

COMPUTATION OF THE PERCENTAGE UNCERTAINTY OF THE SLOPE
OF EACH CURVE IN FIGURE 19

Curve[a]	$\frac{dA}{dt}$	S[b]	$A_n - A_1$[c]	Percentage uncertainty of $\frac{dA}{dt}$[d]
1	0.0060	0.0009	0.105	1.7
2	0.0049	0.0055	0.240	4.6
3	0.0051	0.0030	0.264	2.3
4	0.0048	0.0026	0.118	4.5
5	0.0047	0.0010	0.151	1.3

[a]The incident photon energy for curves 1, 2, and 3 was 13.4 keV and for curves 4 and 5 was 14.1 keV.

[b]
$$S = \sqrt{\sum_{i=1}^{n} \frac{|A_i - A(t_i)|^2}{n}}$$, where $A_i - A(t_i)$ is the deviation of the experimental point, A_i, at t_i from the value, $A(t_i)$, determined from the curve; and n is the number of experimental points.

[c]$A_n - A_1$ is the total change in absorbance between the first and the last points of the curves in Figure 19.

[d]The percentage uncertainty of $\frac{dA}{dt}$ is $\frac{2S}{A_n - A_1} \times 100$.

TABLE 6

COMPUTATION OF THE PERCENTAGE UNCERTAINTY IN $\left[\dfrac{dA}{dt}\right]_{13.4\ keV}$ OBTAINED FROM FIGURE 19

Curve	Slope, $\dfrac{dA}{dt}$ (hours^{-1})	Average value of the slope	Deviation from the average	Standard deviation of the average	Percentage deviation of the average
1	0.0060		7×10^{-4}		
2	0.0049	0.0053	4×10^{-4}	3.4×10^{-4}	6.4%
3	0.0051		2×10^{-4}		

larger than ± 2 percent. This fact refers only to the uncertainty in the knowledge that the energy fluxes were the same in the runs in which 13.4 keV photons were used as in the runs in which 14.1 keV photons were used. Another uncertainty that would affect the knowledge of the equality of the energy fluxes arises from the estimated values for the mass absorption coefficient of air at 13.4 keV and at 14.1 keV. However, this error is primarily systematic. An additional random uncertainty originates from the readings of the curve of mass absorption coefficient as a function of photon energy. This uncertainty is assumed to be smaller than one percent, and is considered negligible.

In the result, $\frac{dF}{dE_i}$, of Equation (5) the uncertainty is the square root of the sum of the squares of the uncertainties in the two experimentally determined quantities, $\frac{dA}{dt}$ and F_i, which are factors in the equation.

The inaccuracy of the optical measurements suggested that the uncertainty in $\frac{dA}{dt}$ is 3 percent. The standard errors of the values of $\frac{dA}{dt}$ which were obtained from the least square fit to each set of experimental points at 14.1 keV suggest that an uncertainty of 2.9 percent is a reasonable estimate. See the entries in Table 5 for curves 4 and 5 of Figure 19. The standard error of the average value of $\frac{dA}{dt}$ which was computed from the least square fit to each set of experimental points at 13.4 keV is 6.4 percent.

See Table 6.

There is an uncertainty of 2 percent in the statement that the runs at 14.1 keV were done at the same energy flux as the runs at 13.4 keV. This estimate of the uncertainty was based on the inaccuracy of the readings of the dosimeter.

Thus, the uncertainty in $\frac{dF}{dE_i}$ at 13.4 keV can be assumed to be 6.4 percent; then, the uncertainty in $\frac{dF}{dE_i}$ at 14.1 keV should be taken as 3.6 percent, obtained from $\sqrt{3^2 + 2^2}$.

Any statement given in units of energy, such as the energy of formation of one F center, contains uncertainties which originate from the calorimetric calibration of the dosimeter and from the use of Smakula's equation, as well as those which originate from the optical measurements and from the readings of the dosimeter.

The uncertainty of the calorimetric calibration of the dosimeter, given in Appendix A, is 2.7 percent. This uncertainty is the standard error of the average of the calorimetric calibrations of the dosimeter for incident photon energies of 13.4 keV, 14.1 keV, 14.9 keV, and 15.7 keV. Furthermore, in the intensity range of the beams used in the experimental work, the calorimeter is expected to give a result with an accuracy of 1 to 3 percent. The estimated uncertainty (2.7 percent) agrees with the inherent accuracy of the calorimeter.

Another uncertainty originates with the constants used in Smakula's equation. For example, the oscillator strength is not satisfactorily known.[116] Also, the experimental determination of the half-width of the F band introduces an uncertainty.

In the measurements on KBr at 300°K and on RbBr at 78°K and at 300°K the optical measurements were less accurate than in the measurements on KBr at 78°K. The variations in absorbance observed during the optical measurements on each sample are as follows: KBr at 78°K, 3 percent; KBr at 300°K, 5 percent; RbBr at 78°K, 10 percent; RbBr at 300°K, 30 to 50 percent; and KCl at 78°K, 1 percent.

Each of the experimental results contains two or more of the uncertainties which have been discussed. A description of each result, together with its uncertainty and its sources of uncertainty, is listed in Table 7.

TABLE 7

SUMMARY OF RESULTS, THEIR UNCERTAINTIES, AND THE SOURCES OF UNCERTAINTY

Result	Uncertainty	Source of uncertainty
1. In KBr at 78°K the rate of formation of F centers per unit <u>absorbed</u> energy is the same whether 13.4 keV or 14.1 keV is the incident photon energy.	6.4%	a
2. Energy of formation of one F center (E_F) in KBr at 78°K	4.4%	a,b,c
3. E_F in KBr at 300°K	5.7%	a,b,c
4. E_F in KCl at 78°K	4.2%	a,b,c
5. E_F in RbBr at 78°K	17%	a
6. E_F in RbBr at 300°K	30%	d

[a] Standard deviation of the average value of the slopes of the growth curves of coloration.

[b] Uncertainty (2%) in the dosimetry.

[c] Uncertainty (2.7%) in the calorimetric calibration of the dosimeter.

[d] Bleaching of the F band during the optical measurements.

IV. DISCUSSION

A. The Function of Halogen K Shell Ionization in the Formation of F Centers in Alkali Halide Crystals

1. The function of bromine K shell ionization in the formation of F centers in KBr

The efficiency of formation of F centers per unit energy absorbed in a KBr crystal while exposed at 78°K to monochromatic X-ray photons of 13.4 keV or 14.1 keV shows no dependence on the incident photon energy. These results are shown in Table 3. They do not support J. Sharma's observation that in KBr the efficiency of formation of F centers per unit incident energy at photon energies just above the halogen K edge is 1.1 times the efficiency of formation at energies just below the K edge.[18]

T. A. Carlson and M. O. Krause indicated that a K shell ionization in bromine would lead to a probability distribution of multiply ionized atoms that would not be significantly different from the probability distribution which would result after an L shell ionization. See Figures 1 and 2. In either a K shell or an L shell

86

ionization, the probability that the bromine loses 4 or more electrons is large.[13] Therefore, even if multiple ionization were significant in the process which leads to F center formation in alkali halides, the energy region around the bromine K edge would not be sensitive to changes in the incident photon energy.

2. The function of chlorine K shell ionization in the formation of F centers in KCl

Carlson and Krause indicated that a K shell ionization in chlorine would result in the loss of a greater number of electrons than an L shell ionization would. The average loss would be: about 4 electrons for a K shell ionization, about 3 electrons for an L_I shell ionization, or about 2 electrons for an L_{II} shell or L_{III} shell ionization.[13]

L. T. Chadderton's computer calculation predicted that the loss of 3 or 4 electrons by a chlorine ion in a KCl lattice would lead to Frenkel defect formation. On the other hand, the same calculation predicted that the loss of 1 or 2 electrons by a chlorine ion in a KCl lattice would not lead to the formation of Frenkel defects.[43]

Sharma found that in KCl the value of the efficiency of formation of F centers per unit incident energy at photon energies above the chlorine K edge is 2.5 times the

efficiency of formation at photon energies below the K edge.[18]

In view of the results of Carlson and Krause, of Chadderton, and of Sharma, the role of halogen multiple ionization in the formation of F centers in KCl should receive additional study. Also, since the intensity of monochromatic radiation produced by a fluorescent technique is higher than that produced by a crystallographic technique, the fluorescent technique should be used in this study.

B. The Mechanism of Formation of F Centers in Alkali Halides

The details of the mechanism by which F centers are formed in alkali halides by ionizing radiation remain to be unraveled. Certainly, the low energy (excitonic) mechanism proposed by D. Pooley and by H. N. Hersh (discussed in Section II-C-5) is successful in explaining luminescent and variable temperature phenomena, as well as ultraviolet radiation damage in alkali halides.[53-57] On the other hand, the insensitivity to K shell ionization that is reported in this thesis does not eliminate the possibility that a multiple ionization of the halogen can lead to F center formation by a Varley-type mechanism.[42,86-88] This possibility exists because no significant change is expected in the probability distribution of ions as the energy of the

incident photons crosses the K edge of bromine, and, therefore, the energy range around the bromine K edge is not significantly sensitive to changes in incident photon energy.

C. The Energy of Formation of One F Center in Each of Several Alkali Halides

The energies of formation of one F center were measured at 78°K in KBr, in KCl, and in RbBr; and at 300°K in KBr and in RbBr. The measurements are listed in Table 4 and agree with previously reported values.[67]

D. The Selective Excitation of a Key Site

When a selectively excited atom contributed a significant percentage to the molecular weight (and hence, to the absorption coefficient) of a system, radiation damage showed no dependence on the photon energy. In this type of interaction the radiation damage appears to be a bulk property of the system.[3,4]

On the other hand, when the excited atom contributed a negligible percentage to the molecular weight (and hence, to the absorption coefficient) of a system, but was located in a structure which significantly affected the property used as a measure of radiation damage, then the damage was sensitive to photon energies in a range which included an

inner ionization edge of the atom. In this type of
interaction the radiation damage depends on where in the
system the energy is absorbed. The damage is greatest when
excitation occurs at the key structure--the sensitive
site.[2,6,8-10]

A doped alkali halide exhibits the conditions that
were present in the systems in which radiation damage is a
function of incident photon energy. Results of experiments
on KI doped with thallium[64,65,118] and KCl doped with
lead[60,61] showed that in certain temperature ranges some
luminescent and color centers are stable only in the
presence of these impurities. Presumably, one or more of
the optical properties of these doped crystals can be
altered by selective damage at the impurity sites--the
sensitive sites.

Since this changeable optical property could be used
as a measure of radiation damage, an alkali halide doped
with a heavy-atom impurity, such as lead or thallium, would
be an excellent system in which to study the possible
dependence of radiation damage on incident photon energy.
Radiation damage should be studied in an energy range which
includes the absorption edges of the dopant. If a dependence
of radiation damage on incident photon energy would be
observed in a well-controlled experiment, this observation
would be a reliable indication that atomic sites exist

which are particularly susceptible to ionizing radiation damage--damage that begins with inner-shell ionization which is followed by an Auger cascade.

E. Conclusion

Ionization in the K shell of bromine in KBr at $78^{\circ}K$ plays no optically detectable role in the formation of F centers.

The energy of formation per F center was found for each of several alkali halides.

The combination of fluorescent excitation of targets and ionization chamber dosimetry is a promising and well-tested technique for the production of monochromatic X-ray beams of varied photon energies but of the same energy flux.

The role of halogen multiple ionization in the formation of F centers in alkali halide crystals should be investigated in KCl. In KCl any dependence of F center formation on the multiple ionization of the halogen ion is expected to be observable.

Present evidence indicates that ionizing radiation damage may not always be a bulk property of a system. In some systems the selective excitation of a sensitive site results in an increased indication of radiation damage.

APPENDIX A

A. Air Ionization Chamber Dosimetry

In the process of calibrating the X-ray beams in
order to obtain the same energy flux on the sample for all of
the incident photon energies, the steps described below were
followed: First, a fluorescent radiator and a filter were
placed as shown in Figure 8. Second, the Victoreen Model 651
Air Ionization Chamber was charged while it was in position
within the Model 570 Condenser R Meter. Third, the Chamber
was centered in the beam in such a way that its window was
in the position occupied by the face of the sample during
irradiation. See Figure 13. Fourth, the X-ray tube was
repeatedly operated for a given time (50 to 100 seconds) at
45 kvp and at each of several current settings; the readings
of the Chamber were recorded after each exposure. Fifth,
the fluorescent radiator and the filter were replaced and
the above procedure was repeated. Sixth, for each
fluorescent radiator used, a graph was made of the Chamber's
readings in roentgens divided by the exposure time and by
the mass absorption coefficient of air (in units of cm^2/gm)
as a function of the current setting in the X-ray tube. See
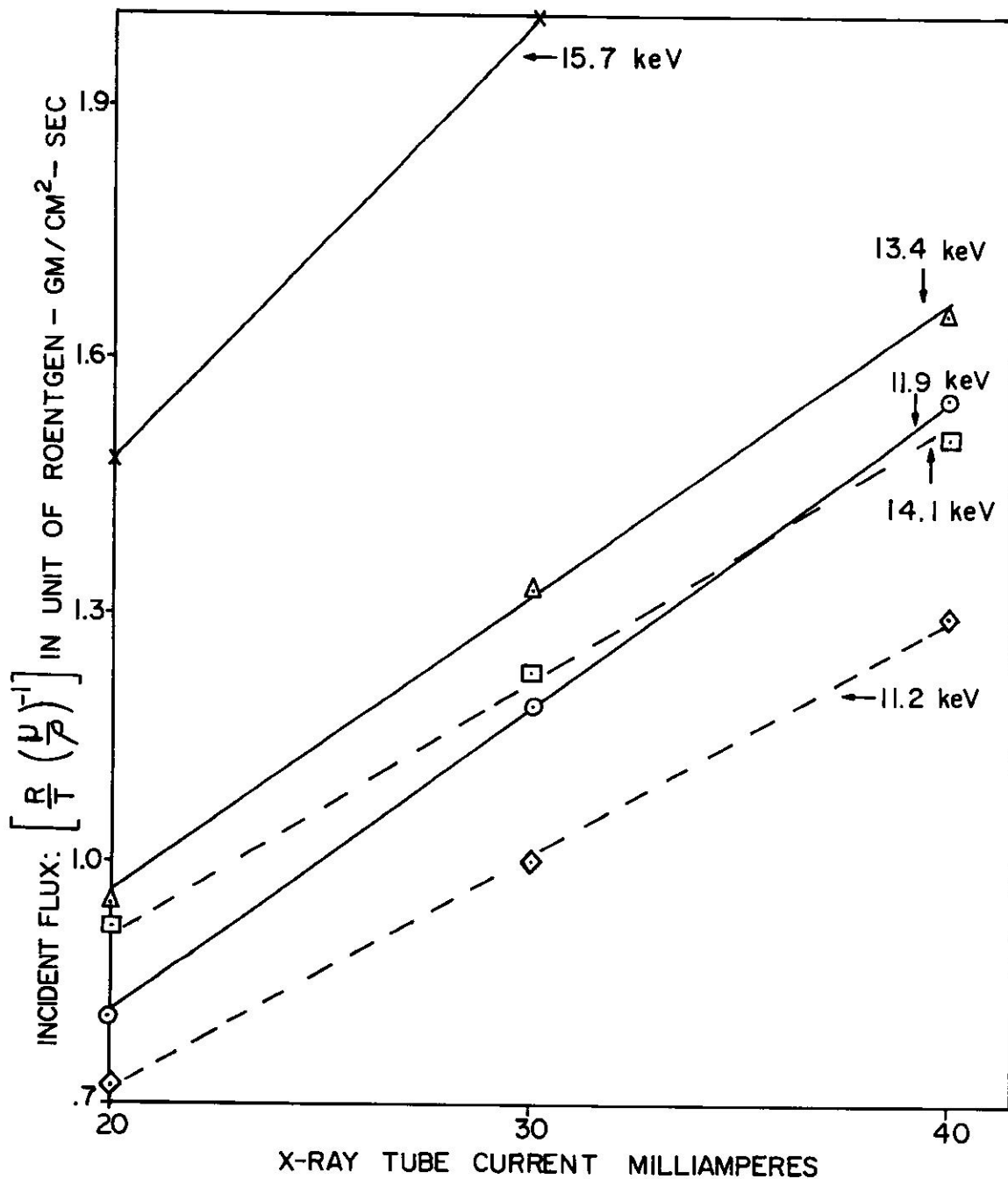Figure 20. (The values used for the mass absorption

92

Figure 20. The incident energy flux on the sample—measured by the Victoreen Dosimeter and plotted as a function of the X-ray tube current at 45 kvp. Each curve is labeled with the energy of the photons incident on the dosimeter. The incident photons are filtered outputs of the fluorescent radiators.

coefficient of air are shown in Table 8.) Seventh, the current setting for each fluorescent radiator was carefully selected so that the incident energy flux (in units of roentgen-gm/cm^2-sec) on the Chamber would be the same for all radiators used.

The process of calibrating the X-ray beam was repeated several times during the course of the experimental work. The calibration was reproducible. Low humidity was essential in order to obtain reliable dosimetry readings. The time of exposure was varied to achieve a reading of 200 ± 20 roentgens regardless of the current setting and the incident photon energy. This procedure was necessary because an exposure half as long as any previous exposure gave a reading approximately 10 percent larger than half the reading of the longer exposure. Thus, the Chamber's efficiency of collecting ions was affected by the voltage difference which remained in the Chamber. Probably, this effect is what caused the curves in Figure 20 to interpolate to points off the origin of coordinates.

A full set of dosimetry measurements was also done in which the face of the Chamber was in the position occupied by the face of the gold target of the calorimeter during calorimetric measurements. These measurements were used to calibrate the dosimetry in units of energy. The curves obtained from these measurements are shown in Figure 21.

TABLE 8

MASS ABSORPTION COEFFICIENT OF AIR[a]

Photon Energy (keV)	μ/ρ (cm^2/gm)
11.2	3.80
11.9	3.10
13.4	2.20
14.1	1.93
14.9	1.63
15.7	1.40

[a]The values were calculated from values given by Compton and Allison, reference 119, for argon, oxygen, and nitrogen. The composition of air was assumed to be 1.3% argon, 23.2% oxygen, and 75.5% nitrogen.
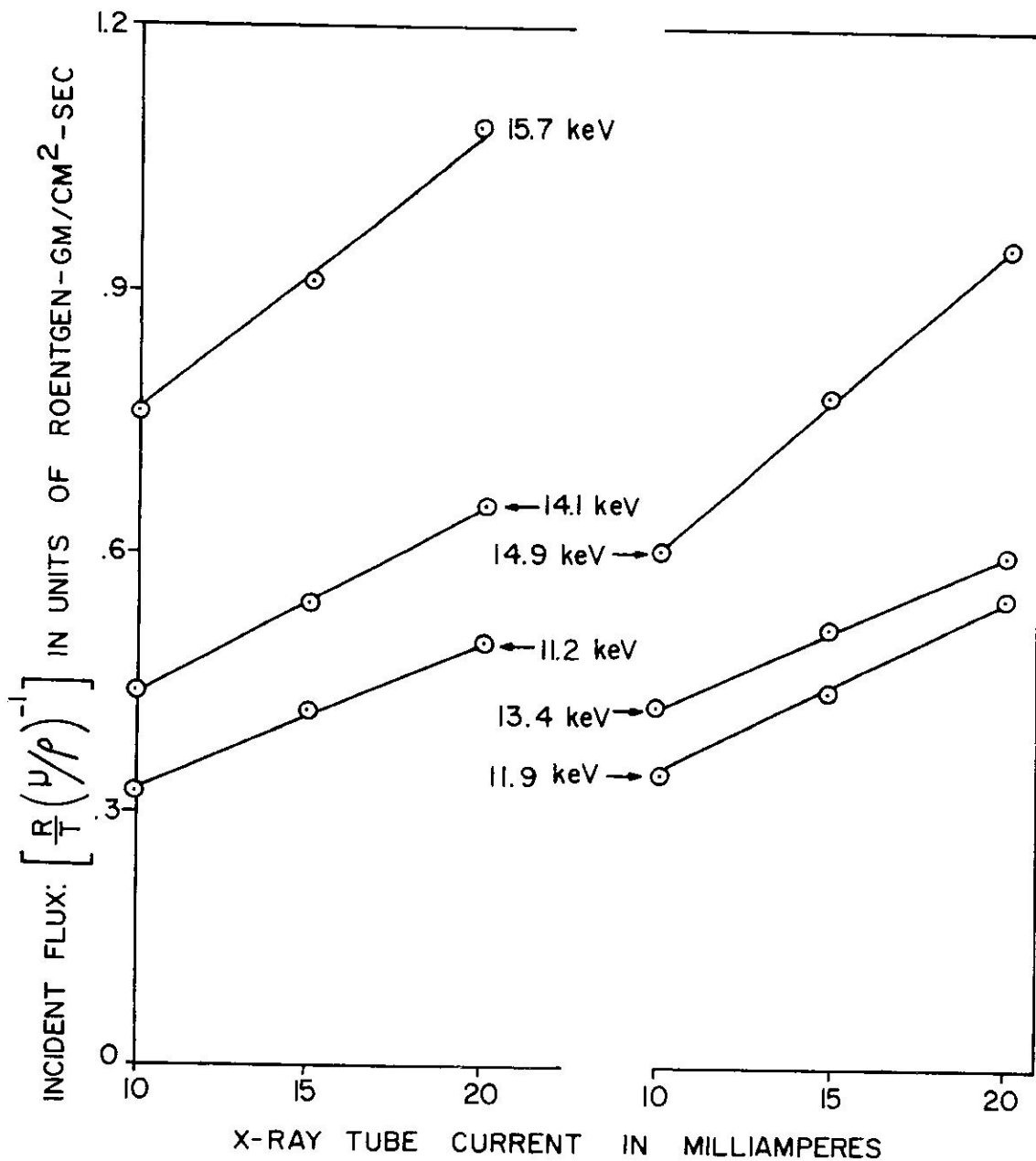
Figure 21. The incident flux on the air ionization chamber when the front of the chamber is at the position of the gold target of the calorimeter--plotted as a function of the X-ray tube current at 45 kvp. For each curve the incident photon energy is shown.

The curves give the readings of the dosimeter, divided by the time of exposure and by the mass absorption coefficient of air, which are plotted against the current in the X-ray tube operated at 45 kvp.

B. Calorimetry

The calorimeter was described in Section III-C. Two thermistors on the back of a totally absorbent double layer of gold foil were connected to opposite branches of a Wheatstone bridge. When radiation was absorbed by the calorimeter, heat from the target brought about a change in the resistance of the thermistors. This caused an imbalance in the Wheatstone bridge. The imbalance was recorded in a fast moving strip-chart recorder; the slope of the signal on the chart changed with a change in the energy absorbed by the target. This change in slope was in turn calibrated in absolute energy units as follows: In the construction of the target a heater wire of known resistance had been coiled between the two layers of gold foil. At a given voltage a known energy would be dissipated as heat by the resistance coil. This would cause an imbalance in the Wheatstone bridge and a corresponding change in slope by the trace of the recorder. Then, this change in slope would be translated to an energy input.

Since the speed of the recorder's chart was limited,

the current settings of the X-ray tube had to be limited to a maximum of 35 milliamps. The accuracy (2 to 4 percent in the readings of the slopes) of the calorimetric measurements at this current setting is less than the accuracy at lower current settings.[111]

Figure 22 shows the curves of the energy flux obtained from each filtered radiator and plotted against the current setting of the X-ray tube at 45 kvp.

For a given radiator (photon energy) the energy equivalent of one roentgen is obtained by dividing a reading from a curve in Figure 22 by the reading at the same value of the current which is obtained from the corresponding curve in Figure 21. Table 9 shows the values obtained for the energy equivalent of one roentgen for several of the photon energies used (13.4 keV, 14.1 keV, 14.9 keV, and 15.7 keV). Table 9 also shows that the average value of the calibrations is 11.3 keV ($\pm$ .3 keV). The uncertainty, $\pm$ .3 keV, is the standard deviation of the average of the values. This uncertainty is approximately equal to the uncertainty (2 percent) of the readings of the slopes of the recorder tracings of the calorimeter.
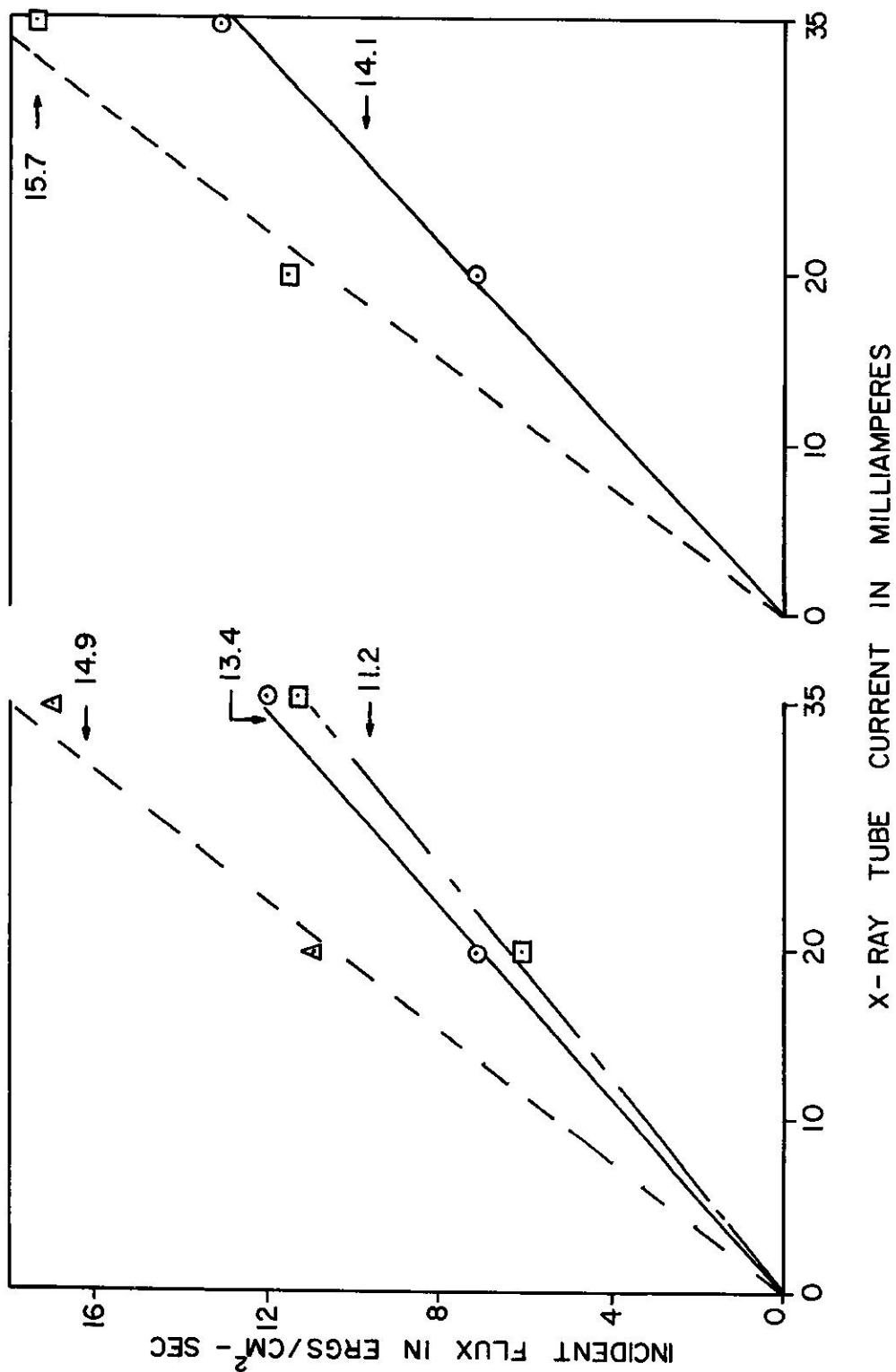
Figure 22. The incident energy flux on the gold target of the calorimeter as a function of the current in the X-ray tube operated at 45 kvp. The energy in keV of the incident photons is given next to each curve.

TABLE 9

THE ENERGY EQUIVALENT OF ONE ROENTGEN MEASURED BY THE VICTOREEN MODEL
651 CHAMBER AND 570 ELECTROMETER[a]

Photon energy (keV)	Dosimetry readings (r-gm/cm²-sec)	Calorimetric readings (ergs/cm²-sec)	Energy equivalent of one roentgen[b] (ergs/r-gm)	Average energy equivalent of one roentgen (ergs/r-gm)
13.4	0.60	7.11	12.1	
14.1	0.65	7.02	11.0	$11.3 \pm .3$[c]
14.9	0.95	11.0	11.7	
15.7	1.06	11.4	10.9	

[a]The readings of the dosimeter and of the calorimeter were obtained with the X-ray tube operated at 45 kvp and at 20 ma. See Figures 21 and 22.

[b]A correction was made for the absorption of a beryllium window 0.002 inches thick which was in the path of the beam when the calorimeter was used.

[c]The uncertainty in this result is the standard deviation of this average.

APPENDIX B

A. Growth Curves of Coloration of Some
Alkali Halides during X-Ray Exposure
at 78°K and at 300°K

During the course of this work several alkali halides were exposed at 78°K and at 300°K to the calibrated X-ray beams. The resulting growth curves of coloration are shown in this appendix. See Figures 23, 24, 25, 26, and 27. The results of the calculation of the values for the energy of formation of one F center are shown in Table 4.

In every case reported in this appendix the crystal was exposed to several incident photon energies. The radiator and the filter (hence, the photon energy) were changed immediately after each optical measurement. Along the top edge of Figures 23 through 27, the incident photon energy (in keV) is given for each exposure.

Throughout this work the X-ray tube was operated at 45 kvp, and the current was varied in order to obtain the same energy flux, 5.77×10^4 ergs/cm^2-hr $\pm 3.3\%$ (3.62×10^{16} eV/cm^2-hr $\pm 3.3\%$), for all photon energies. The value of the energy flux was obtained by substituting the experimentally determined value of the incident flux, $\dfrac{R}{(\mu/\rho)t} = 1.46$ roentgen-gm/cm^2-sec $\pm 2\%$, in Equation (1).

Figure 23. Absorbance at the peak of the F band of KBr irradiated at 78°K--as a function of exposure time. For each exposure the energy in keV of the incident photons is shown at the top. The incident energy flux was the same throughout the run. The straight line is the least square fit to the experimental points through which the line is drawn.

Figure 24. Absorbance at the peak of the F band of KBr irradiated at 300°K--plotted as a function of exposure time. For each exposure the energy in keV of the incident photons is shown at the top. The incident energy flux was the same throughout the run. The straight line is the least square fit to the experimental points through which the line is drawn.

Figure 25. Absorbance at the peak of the F band of KCl irradiated at 78°K--plotted as a function of exposure time. For each exposure the energy in keV of the incident photons is shown at the top. The incident energy flux was the same throughout the run. The straight line is the least square fit to the experimental points through which the line is drawn. No correction was made for the transmitted flux, but for each photon energy the percentage of the incident flux absorbed in the crystal (0.74 cm thick) is shown in the inset.
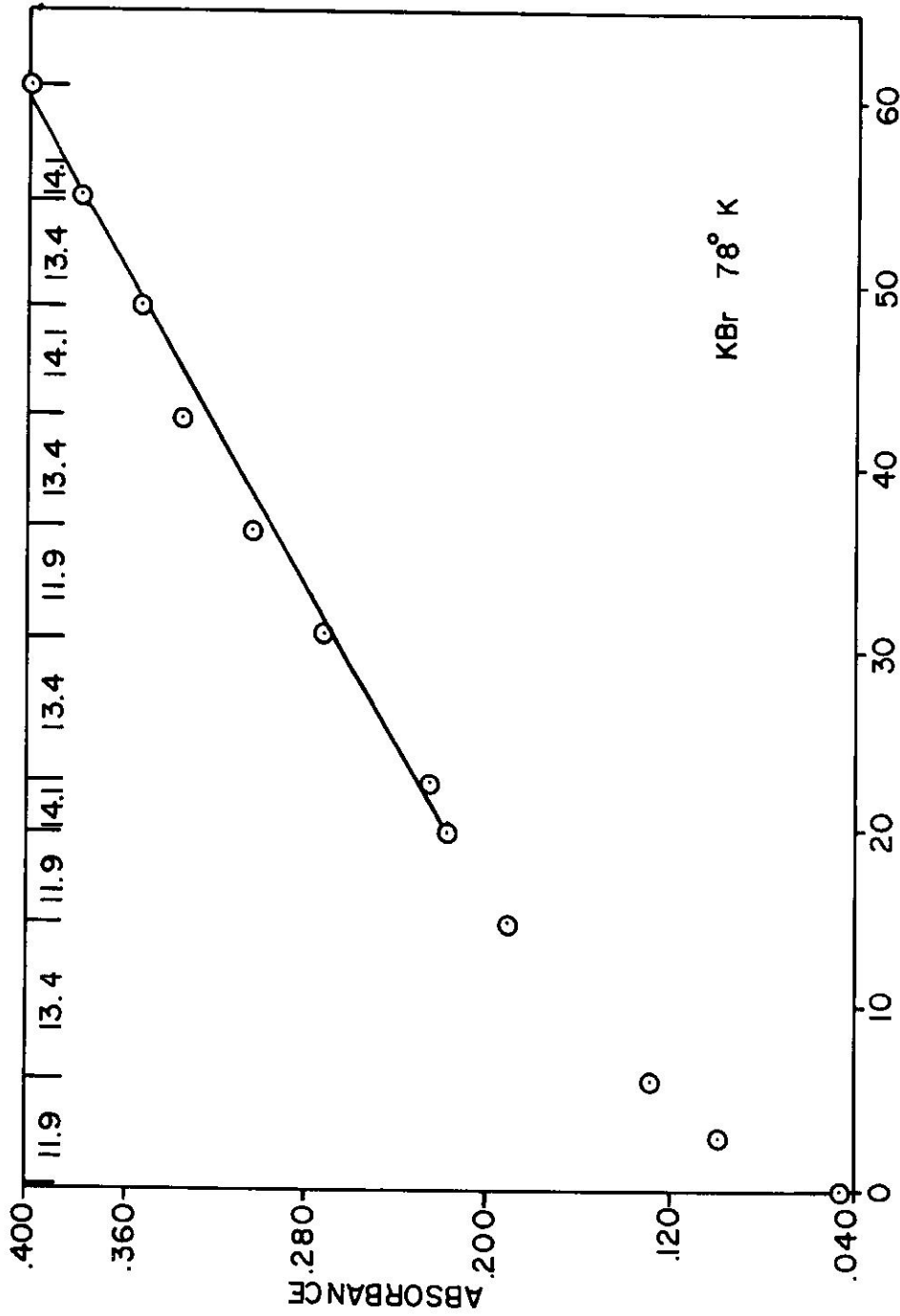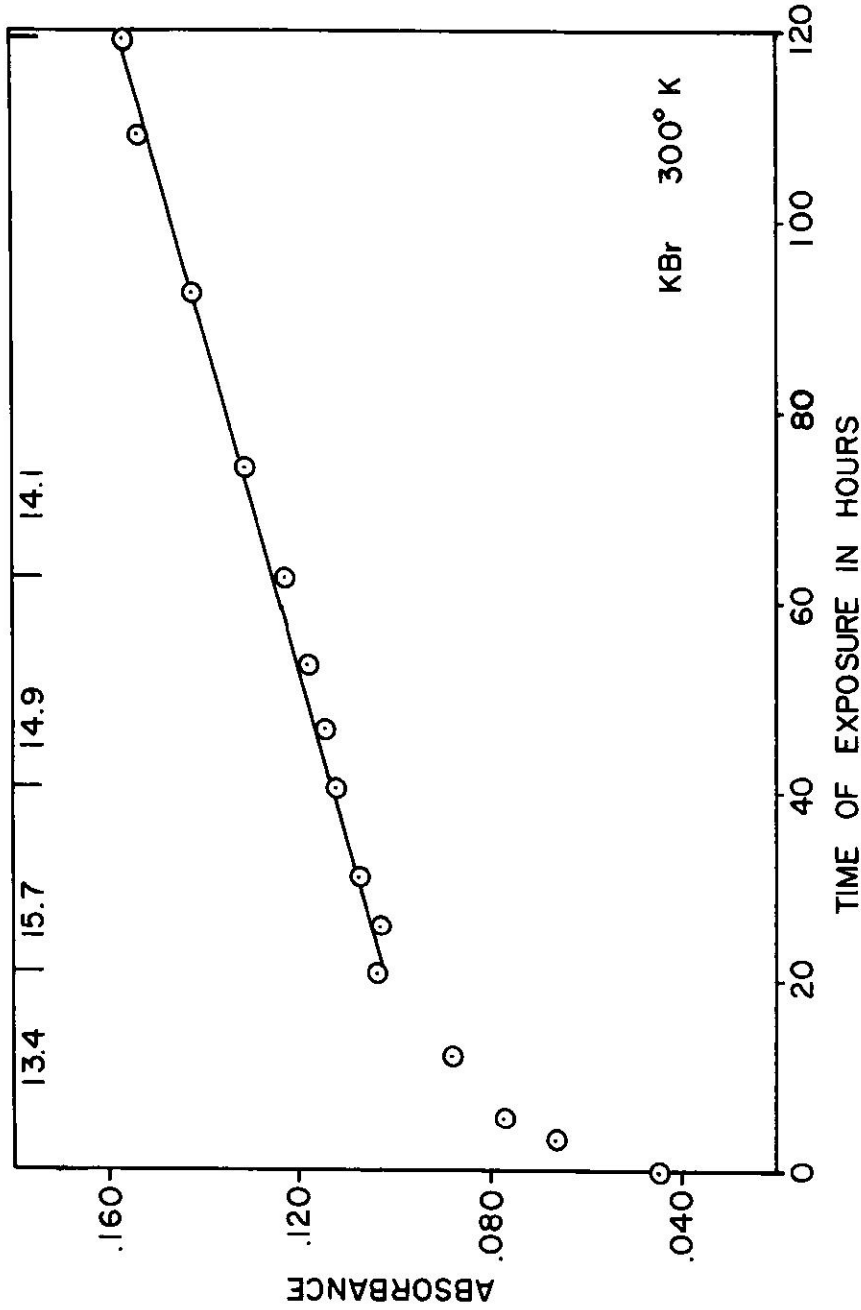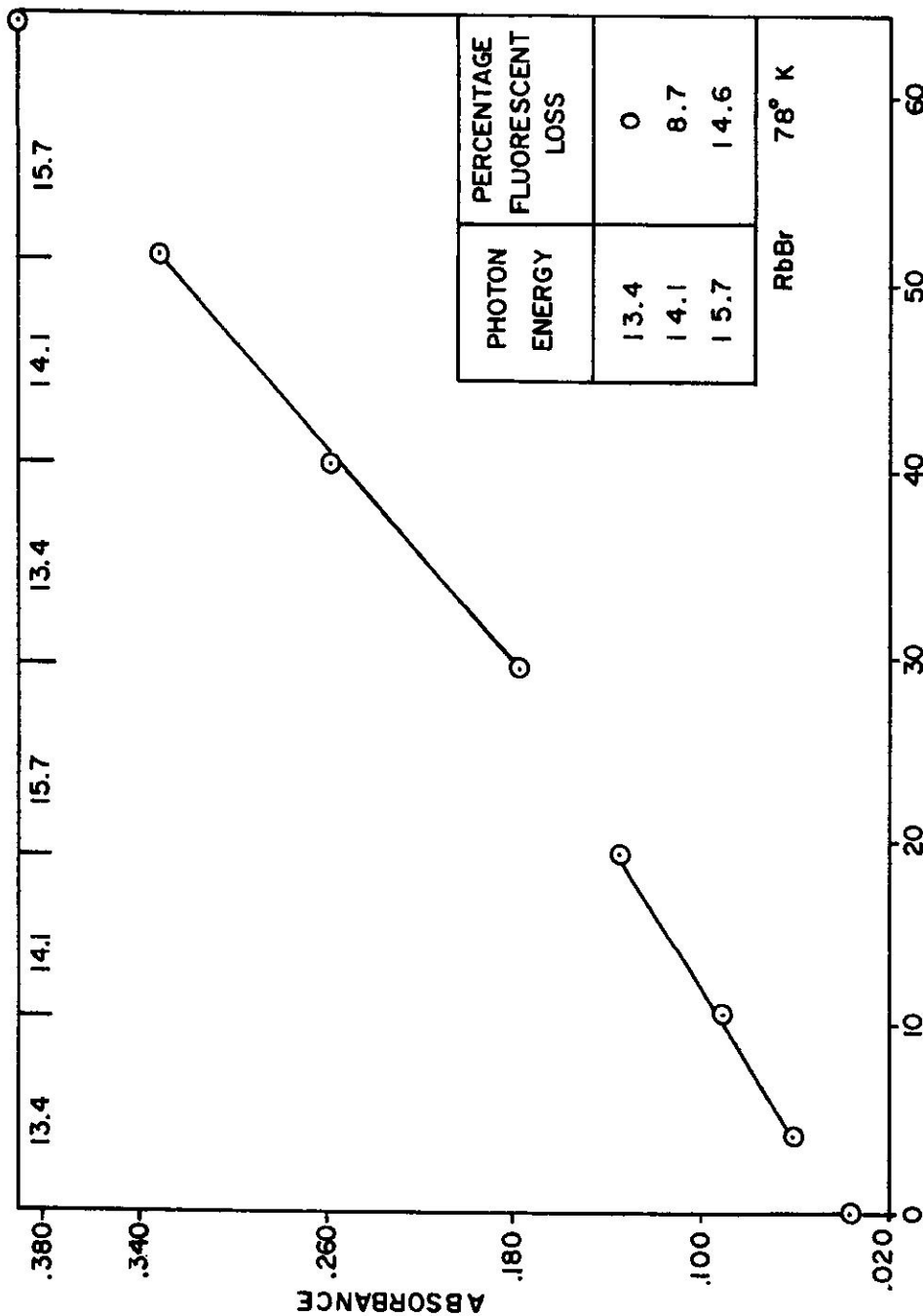
Figure 26. Absorbance at the peak of the F band of RbBr irradiated at 78°K--as a function of exposure time. For each exposure the energy in keV of the incident photons is shown at the top. The incident energy flux was the same throughout the run. Each of the two straight lines is the least square fit to th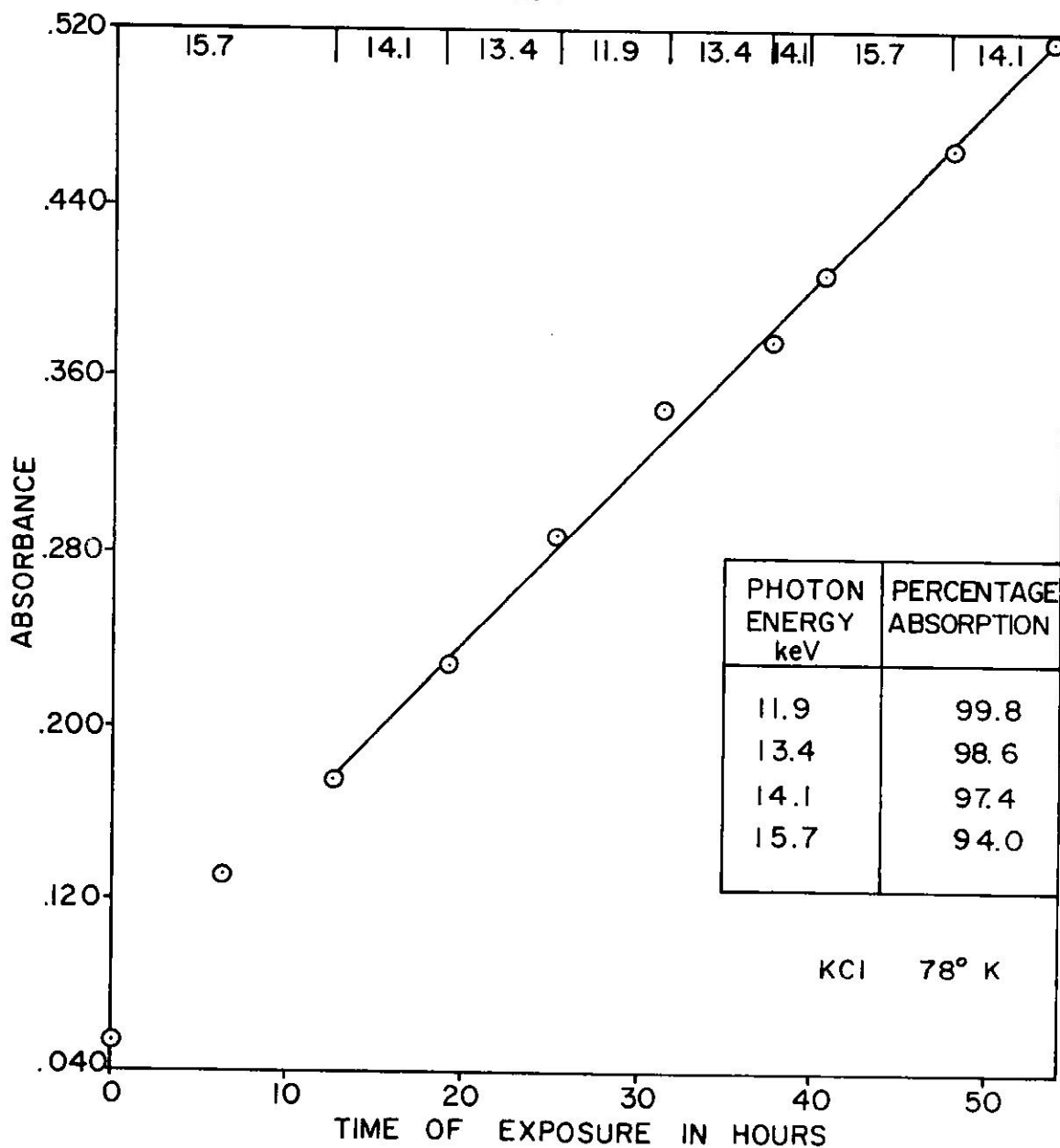e set of experimental points through which the line is drawn. The percentage of the incident flux lost from the crystal by fluorescence is shown in the inset.
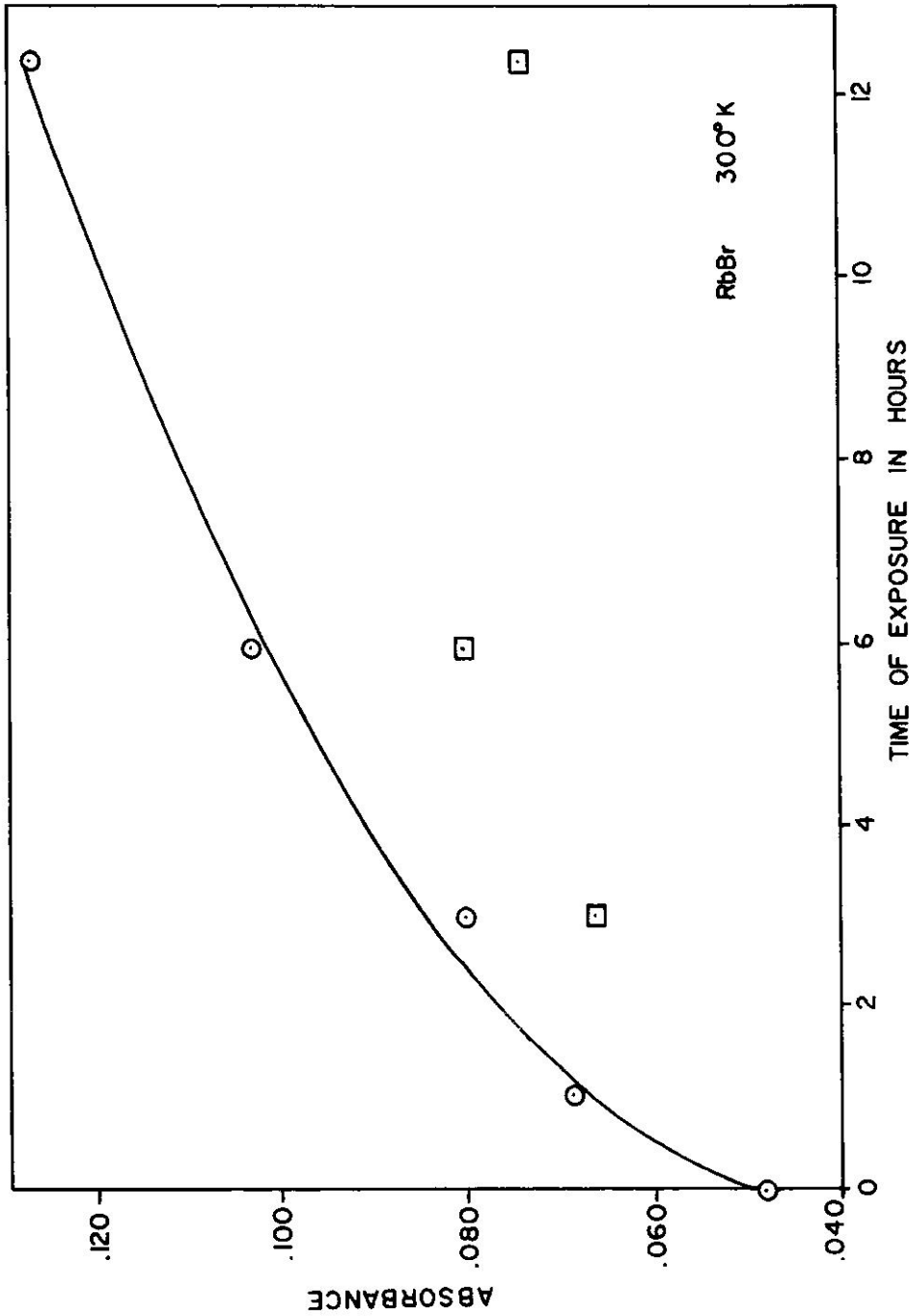
Figure 27. Absorbance at the peak of the F band of RbBr irradiated with 13.4 keV photons at 300°k--plotted as a function of exposure time. The absorbance measurements in circles were taken immediately after the sample had been removed from the beam. The measurements in squares were taken 2 to 3 minutes later. The interval between these two sets of experimental points indicates the amount of bleaching during the optical measurements. The solid line suggests a growth curve.

(See page 53.)

In each run the sample was in the position identified
in Appendix A as the sample position for 78°K irradiations.
Even for the runs at 300°K the samples were in that position.
Thus, for all runs the dosimetry curves of Figure 20 are
applicable.

For KCl at 78°K the calculation of the energy of
formation of one F center assumes that Smakula's equation
for the rate of formation of F centers (per square centimeter
per unit time) is

$$\left[\frac{d(Nd)}{dt}\right]_{KCl,\ 78°K} = 6.22 \times 10^{15} \frac{dA}{dt}$$

In the computation of the constant in this equation the
following values were used: 0.80 for the oscillator strength,
f; 0.20 eV for the half-width, W, of the F band; and 1.49 for
the index of refraction, n. (See Section III-E)

Then, for KCl at 78°K the efficiency of formation of
F centers is

$$\frac{dF}{dE_i} = \frac{6.22 \times 10^{15}}{F_i} \frac{dA}{dt}$$

$$= 1.08 \times 10^{11} \frac{dA}{dt} \text{ ergs}^{-1} \pm 4.2\%$$

$$\frac{dF}{dE_i} = 0.172 \frac{dA}{dt} \, eV^{-1} \pm 4.2\%$$

(See Section III-H-1) In the calculation of the uncertainty the standard deviation (2.6%) in the estimate of the value of the slope of the curve in Figure 25, the uncertainty (2%) in the dosimetry, and the uncertainty (2.7%) in the calorimetry were considered.

The values of the slopes, $\frac{dA}{dt}$, of the curves in Figures 24, 25, 26, and 27 are shown in Table 10. The curves in Figures 24, 25, and 26 are the least square straight lines fit to the experimental points through which the lines are drawn.

TABLE 10

RATE OF CHANGE OF ABSORBANCE OF SOME ALKALI HALIDES
DURING EXPOSURE TO X RAYS AT $78^\circ K$ OR $300^\circ K$

Alkali halide	Temperature of exposure	Figure reference	$\frac{dA}{dt}$ (hours^{-1})
KBr	$78^\circ K$	19	$5.3 \times 10^{-3} \pm 3.5\%$[a]
KBr	$300^\circ K$	24	$5.7 \times 10^{-4} \pm 4.6\%$[b]
KCl	$78^\circ K$	25	$8.2 \times 10^{-3} \pm 2.6\%$[b]
RbBr	$78^\circ K$	26	$5.9 \times 10^{-3} \pm 17\%$[c]
RbBr	$300^\circ K$	27	$2.3 \times 10^{-3} \pm 30\%$[d]

[a]The uncertainty in this result is the standard deviation of the average of the slopes of the five curves in Figure 19.

[b]The uncertainty in this result is the standard deviation of the estimate of the slope of the curve in Figure 24.

[c]This result is the average of the slopes of the two line segments in Figure 26. The slopes of the line segments are 4.9×10^{-3} hours^{-1} and 6.9×10^{-3} hours^{-1}. The uncertainty in this result is the standard deviation of the average of these two values.

[d]The uncertainty in this result was estimated on the basis of the change in absorbance during the optical measurements.

APPENDIX C

A. Correction due to K Shell Fluorescence

In the discussion that follows, the percentage of energy lost by fluorescence from a slab which is exposed to a photon energy larger than the K absorption energy of an element in the slab is derived in a general form. This derivation closely follows the calculation by W. J. Veigele and N. J. Roper.[117]

Let F_i be the flux incident on the slab of Figure 28. Let $h\nu_i$ be the energy of the incident photons, and let μ_i be the absorption coefficient of the slab at that energy. Then, the rate, $\frac{dS}{dt}$, of photon absorption in area da' in layer dx' at x' is

$$\frac{dS}{dt} = \mu_i \left[\frac{F_i}{h\nu_i} \right] \left[\exp(-\mu_i x') \right] dx' da' \ .$$

When the incident photon energy is larger than the K absorption energy, the fraction of photons absorbed in the K shell is
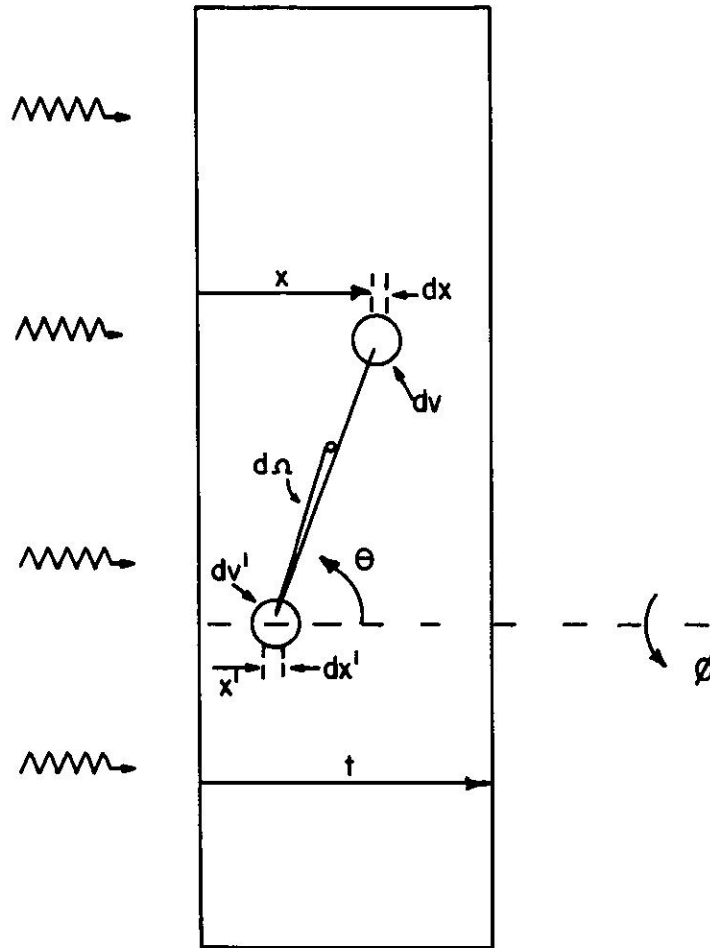
Figure 28. Coordinate system for the calculation of fluorescence in a slab. After Veigele and Roper, reference 117.

$$\frac{\Delta(\mu/\rho)_{K \text{ edge}}}{(\mu/\rho)_>} = \frac{r_K - 1}{r_K} ,$$

where $\Delta(\mu/\rho)_K = (\mu/\rho)_> - (\mu/\rho)_<$ is the change in the mass absorption coefficient as the K edge is crossed, $(\mu/\rho)_>$ is the mass absorption coefficient above the K edge, and $(\mu/\rho)_<$ is the mass absorption coefficient below the K edge. The K jump ratio, $r_K = \frac{(\mu/\rho)_>}{(\mu/\rho)_<}$, is the ratio of the mass absorption coefficients, one from each side of the K edge.

The fluorescent yield, $\tilde{\omega}_K$, is defined as the fraction of atoms which fluoresces after the atoms have been ionized in the K shell.[19] Each of these atoms emits a fluorescent photon of energy $h\nu_f$. Thus, the rate of energy emission, $\frac{dE}{dt}$, by fluorescence into solid angle $d\Omega$ from volume $da'dx'$ at depth x' is

$$\frac{dE}{dt} = \frac{d\Omega}{4\pi} \left[\frac{r_K - 1}{r_K}\right] \tilde{\omega}_K h\nu_f \left[\frac{\mu_i F_i}{h\nu_i}\right] \exp(-\mu_i x')dx'da' .$$

At point $(x-x', \theta)$ the energy flux which arises from fluorescence in volume $dx'da'$ is equal to $\frac{dE}{dtda'} \exp\left[-\mu_f(x-x')\sec\theta\right]$, where μ_f is the absorption coefficient of the slab at the energy of the fluorescent photons.

Some of the fluorescent emission occurring in a direction such that $x < x'$ ($\frac{\pi}{2} < \theta < \pi$) leads to a fluorescent loss through the face of the crystal exposed to the incident energy flux. Thus, the fluorescent energy flux, F_f, lost through the front face is

$$F_f = \frac{1}{4\pi}\left[\frac{r_K - 1}{r_K}\right]\tilde{\omega}_K h\nu_f \frac{\mu_i F_i}{h\nu_i}\int_0^{2\pi} d\phi$$

$$\times \int_{\pi/2}^{\pi} \sin\theta\, d\theta \int_x^t dx' \exp\left[-\mu_i x' - \mu_f(x-x')\sec\theta\right],$$

where the integral must be evaluated at $x = 0$. The ratio of the fluorescent flux lost through the front face to the incident flux is

$$\frac{F_f}{F_i} = \frac{C\mu_i}{h\nu_i}\int_{\pi/2}^{\pi} \frac{\sin\theta\, d\theta\left[\exp(-\mu_i t + \mu_f t \sec\theta) - 1\right]}{\mu_f \sec\theta - \mu_i}, \qquad (8)$$

where C is given by

$$C = \frac{\tilde{\omega}_K}{2}\left[\frac{r_K - 1}{r_K}\right]\left[h\nu_f\right].$$

For a slab of infinite thickness ($t = \infty$) the fraction of the incident flux that is lost as fluorescence through the front face is

$$\frac{F_f}{F_i} = \frac{C}{h\nu_i} \frac{\mu_i}{\mu_f} \int_{\pi/2}^{\pi} \frac{\cos\theta \, d(\cos\theta)}{1 - \frac{\mu_i}{\mu_f}\cos\theta} = \frac{C}{h\nu_i} \frac{\mu_f}{\mu_i} \int_0^{-\frac{\mu_i}{\mu_f}} \frac{u \, du}{1 - u} \, ,$$

where $u = \frac{\mu_i}{\mu_f}\cos\theta$. After evaluation $\frac{F_f}{F_i}$ becomes

$$\frac{F_f}{F_i} = \frac{C}{h\nu_i} \left[1 - \frac{\mu_f}{\mu_i} \log(1 + \frac{\mu_i}{\mu_f}) \right] . \tag{9}$$

For an infinitely thick KBr crystal exposed to incident photons of 14.1 keV, $\frac{F_f}{F_i}$ is equal to 0.102--obtained by using the following values in Equation (9):
$(\mu/\rho)_> = 124.5 \text{ cm}^2/\text{gm}$, $(\mu/\rho)_< = 25.5 \text{ cm}^2/\text{gm}$, $(\frac{r_K - 1}{r_K} = 0.87)$, $h\nu_f = 11.9$ keV, $\bar{\omega}_K = 0.56$, (C = 2.65 keV), $h\nu_i = 14.1$ keV, $\mu_i = 305 \text{ cm}^{-1}$, and $\mu_f = 102 \text{ cm}^{-1}$.

A computer calculation using Equation (8) for a KBr crystal of thickness t = 0.5 mm has given a result identical to the one obtained from Equation (9). Therefore, since the crystals used in this research were between 0.5 and 0.8 mm thick, the use of Equation (9) is justified.

Some of the emission from the volume da'dx' into the hemisphere $0<\theta<\frac{\pi}{2}$ (x>x') results in a transmitted fluorescent loss, F_t, through the back face (x = t) of the slab:

$$F_t = \frac{F_i C \mu_i}{h \nu_i} \left[\exp(-\mu_i t) \right] \int_0^{\pi/2} \frac{1 - \exp(\mu_i t - \mu_f t \sec\theta)}{\mu_f \sec\theta - \mu_i} \sin\theta d\theta .$$

However, for a KBr crystal 0.5 mm to 0.8 mm thick the result of the above integration is essentially equal to zero.

The results given by Equation (9) for KBr, as well as for RbBr, exposed to 14.1 keV, 14.9 keV, or 15.7 keV photons are shown in Table 11.

TABLE 11

PERCENTAGE OF THE INCIDENT ENERGY FLUX LOST BY
FLUORESCENCE THROUGH THE FACE OF INCIDENCE OF
A KBr OR A RbBr CRYSTAL DURING EXPOSURE TO
MONOCHROMATIC X RAYS

Incident photon energy (keV)	Percentage of the incident energy flux which is lost by fluorescence through the front face of the crystal	
	KBr	RbBr
13.4	0	0
14.1	10.2	8.7
14.9	9.1	7.9
15.7	7.9	14.6

LIST OF REFERENCES

1. J. Garsou, "Contribution a l'etude de l'efficacite des rayons monochromatiques sur quelques systemes d'halogenures organiques solides et liquides." Unpublished Ph.D. dissertation, University of Liege, Belgium, 1959.

2. A. H. Emmons, "Resonance Radiation Effects of Low Energy Monochromatic X Rays on Catalase." Unpublished Ph.D. dissertation, Department of Nuclear Engineering, University of Michigan, 1960.

3. M. C. Atkins, "The Energy Dependence of X-Ray Damage in an Organic Mercury Compound." Unpublished Ph.D. dissertation, Department of Nuclear Engineering, University of Michigan, 1960.

4. W. R. Clendinning, "A Study of the Free Radical Yield Produced in 1-Bromobutane by Irradiation with Monochromatic X Rays of Differing Photon Energies." Unpublished Ph.D. dissertation, Department of Nuclear Engineering, University of Michigan, 1960.

5. W. F. Wegst, "Wavelength Dependent Effects of Low Energy X Rays on Mammalian Tissue Cells." Unpublished Ph.D. dissertation, Department of Environmental Health, University of Michigan, 1963.

6. P. Paraskevoudakis, "Wavelength-Dependence of Horseradish Peroxidase Inactivation by Soft X Rays." Unpublished Ph.D. dissertation, Department of Environmental Health, University of Michigan, 1964.

7. J. W. Baum, "Catalase Inactivation by 4.9 to 7.5 keV Fluorescent X Rays." Unpublished Ph.D. dissertation, Department of Environmental Health, University of Michigan, 1964.

8. H. J. Gomberg, R. A. Luse, and F. Vazquez-Martinez, Resonance in Radiation Effects: Technical Report No. 1. Puerto Rico Nuclear Center 12, University of Puerto Rico, AEC Contract No. AT(40-1)-1833, January, 1963.

9. H. J. Gomberg, R. A. Luse, F. Vazquez-Martinez,
    F. S. Koo, R. J. Santiago de Morales, and
    B. A. Cruz-Vidal, Resonance in Radiation Effects:
    Technical Report No. 2. Puerto Rico Nuclear
    Center 40, University of Puerto Rico, AEC Contract
    No. AT(40-1)-1833, May, 1964.

10. H. J. Gomberg, R. A. Luse, F. S. Koo,
    P. Paraskevoudakis, F. Vazquez-Martinez, and
    B. A. Cruz-Vidal, Resonance in Radiation Effects:
    Technical Report No. 3. Puerto Rico Nuclear
    Center 69, University of Puerto Rico, AEC Contract
    No. AT(40-1)-1833, June, 1965.

11. M. C. Atkins and W. R. Clendinning, Sources of
    Monochromatic X Radiation: Technical Report No. 3.
    UMRI Project 03049, Phoenix Memorial Project,
    University of Michigan, AEC Contract
    No. AT(11-1)-684, 1960.

12. H. J. Gomberg, M. C. Atkins, W. R. Clendinning,
    A. A. Gordus, Soft X-Ray Irradiation Techniques:
    Progress Report No. 3. ORA 3049-3-P, Phoenix
    Memorial Project, University of Michigan,
    AEC Contract No. AT(11-1)-684, December, 1961.

13. T. A. Carlson, W. E. Hunt, and M. O. Krause,
    Phys. Rev. 151, 41 (1966).

14. T. A. Carlson and R. M. White, Proceedings of a
    Symposium on Chemical Effects in Nuclear
    Transformation, Austria, 1965. Vienna:
    International Atomic Energy Agency, 1965, I, 23.

15. T. A. Carlson and R. M. White, J. Chem. Phys. 44,
    4510 (1966).

16. J. H. Schulman and W. D. Compton, Color Centers in
    Solids. New York: The MacMillan Company, 1962,
    chapter vii.

17. Reference 16, p. 29.

18. J. Sharma and R. Smoluchowski, Phys. Rev. 137, A259
    (1965).

19. E. H. S. Burhop, The Auger Effect and Other
    Radiationless Transitions. Cambridge: University
    Press, 1952.

20. A. H. Snell and F. Pleasonton, Phys. Rev. 100, 1396 (1955).

21. A. H. Snell and F. Pleasonton, Phys. Rev. 102, 1419 (1956).

22. A. H. Snell and F. Pleasonton, Phys. Rev. 107, 740 (1957).

23. A. H. Snell and F. Pleasonton, Phys. Rev. 111, 1338 (1958).

24. A. H. Snell and F. Pleasonton, J. Phys. Chem. 62, 1377 (1958).

25. T. A. Carlson, J. Chem. Phys. 32, 1234 (1960).

26. T. A. Carlson and R. M. White, J. Chem. Phys. 36, 2883 (1962).

27. T. A. Carlson and R. M. White, J. Chem. Phys. 38, 2075 (1963).

28. T. A. Carlson and R. M. White, J. Chem. Phys. 38, 2930 (1963).

29. T. A. Carlson and R. M. White, J. Chem. Phys. 39, 1748 (1963).

30. M. O. Krause, M. L. Vestal, W. H. Johnston, and T. A. Carlson, Phys. Rev. 133, A385 (1964).

31. M. O. Krause and T. A. Carlson, Phys. Rev. 149, 52 (1966).

32. T. A. Carlson and M. O. Krause, Phys. Rev. 137, A1655 (1965).

33. T. A. Carlson and M. O. Krause, Phys. Rev. Letters 14, 390 (1965).

34. T. A. Carlson, Phys. Rev. 129, 2220 (1963).

35. T. A. Carlson, Phys. Rev. 130, 2361 (1963).

36. T. A. Carlson, Phys. Rev. 131, 676 (1963).

37. T. A. Carlson and M. O. Krause, Phys. Rev. 140, A1057 (1965).

38. R. E. Howard and R. Smoluchowski, Phys. Rev. 116, 314 (1959).

39. D. L. Dexter, Phys. Rev. 118, 934 (1960).

40. R. E. Howard, S. Vosko, and R. Smoluchowski, Phys. Rev. 122, 1406 (1961).

41. F. E. Williams, Phys. Rev. 126, 70 (1962).

42. J. H. O. Varley, J. Phys. Chem. Solids 23, 985 (1962).

43. L. T. Chadderton, D. V. Morgan, and I. McC. Torrens, Phys. Letters 20, 329 (1966).

44. R. L. Platzman, Symposium on Radiobiology, ed. Nickson, New York: Wiley, 1952, chapter vii.

45. J. Durup and R. L. Platzman, Discussions Faraday Soc. 31, 156 (1961).

46. R. Smoluchowski and D. A. Wiegand, Discussions Faraday Soc. 31, 151 (1961).

47. J. H. Schulman and W. D. Compton, Color Centers in Solids. New York: The MacMillan Company, 1962.

48. J. J. Markham, F Centers in Alkali Halides. New York: Academic Press, 1966.

49. Reference 47, p. 28.

50. Reference 48, chapter vi.

51. Reference 47, chapter iv.

52. W. Kanzig and T. O. Woodruff, J. Phys. Chem. Solids 9, 70 (1958).

53. J. D. Konitzer and H. N. Hersh, J. Phys. Chem. Solids 27, 771 (1966).

54. H. N. Hersh, Phys. Rev. 148, 928 (1966).

55. D. Pooley, Solid State Comm. 3, 241 (1965).

56. D. Pooley, Proc. Phys. Soc. (London) 87, 245 (1966).

57. D. Pooley, Proc. Phys. Soc. (London) 87, 257 (1966).

58. A. J. Dekker, Solid State Physics. Englewood Cliffs, New Jersey: Prentice Hall, Inc., 1957, p. 65.

59. Reference 47, p. 220.

60. W. A. Sibley, E. Sonder, and C. T. Butler, Phys. Rev. 136, A537 (1964).

61. E. Sonder and W. A. Sibley, Phys. Rev. 140, A539 (1965).

62. C. J. Delbecq, W. Hayes, M. C. M. O'Brien, and P. H. Yuster, Proc. Roy. Soc. (London) 271, 243 (1963).

63. C. J. Delbecq, A. K. Ghosh, and P. H. Yuster, Phys. Rev. 151, 599 (1966).

64. R. G. Kaufman and W. B. Hadley, J. Chem. Phys. 44, 1311 (1966).

65. W. B. Hadley, S. Polick, R. G. Kaufman, and H. N. Hersh, J. Chem. Phys. 45, 2040 (1966).

66. A. Behr and W. Waidelich, Phys. Letters 23, 620 (1966).

67. H. Rabin and C. C. Klick, Phys. Rev. 117, 1005 (1960).

68. W. H. Duerig and J. J. Markham, Phys. Rev. 88, 1043 (1952).

69. F. Seitz, Revs. Modern Phys. 26, 7 (1954).

70. F. Seitz, Phys. Rev. 80, 239 (1950).

71. Reference 47, p. 25.

72. W. Kanzig, Phys. Rev. Letters 4, 117 (1960).

73. W. Kanzig, J. Phys. Chem. Solids 17, 80 (1960).

74. N. Itoh, B. S. H. Royce, and R. Smoluchowski, Phys. Rev. 137, A1010 (1965).

75. D. L. Dexter, Phys. Rev. 93, 984 (1954).

76. H. Rabin, Phys. Rev. 116, 1381 (1959).

77. F. W. Young and J. H. Crawford, J. Appl. Phys. 31, 1688 (1960).

78. Z. Gyulai and D. Hartly, Z. Physik 51, 378 (1928).

79. H. N. Hersh and J. J. Markham, J. Chem. Phys. Solids 12, 207 (1960).

80. Reference 47, chapter vi.

81. I. Estermann, W. J. Leivo, and O. Stern, Phys. Rev. 75, 627 (1949).

82. K. Sakaguchi and T. Suita, Tech. Repts. of Osaku Univ. 2, No. 43, 177 (1952).

83. L. Lin, Phys. Rev. 102, 968 (1956).

84. C. R. Berry, Phys. Rev. 98, 934 (1955).

85. H. Peisl, R. Balzer, and W. Waidelich, Phys. Rev. Letters 17, 1129 (1966).

86. J. H. O. Varley, Nature 174, 886 (1954).

87. J. H. O. Varley, J. Nuclear Energy 1, 130 (1954).

88. J. H. O. Varley, J. Phys. Chem. Solids 23, 985 (1962).

89. M. H. Cohen, W. Kanzig, and T. O. Woodruff, Phys. Rev. 108, 1096 (1957).

90. W. Kanzig, Phys. Rev. Letters 4, 117 (1960).

91. W. Kanzig, J. Phys. Chem. Solids 17, 80 (1960).

92. V. H. Ritz, Phys. Rev. 142, 505 (1966).

93. H. Ruchardt, Z. Physik 140, 547 (1955).

94. H. Ruchardt, Phys. Rev. 103, 873 (1956).

95. C. C. Klick and D. A. Patterson, Phys. Rev. 130, 2169 (1963).

96. V. H. Ritz, Phys. Rev. 133, A1452 (1964).

97. C. C. Klick, Phys. Rev. 120, 760 (1960).

98. W. Kanzig and T. O. Woodruff, Phys. Rev. 109, 220 (1958).

99. W. D. Compton and C. C. Klick, Phys. Rev. 110, 349 (1958).

100. J. D. Konitzer and J. J. Markham, J. Chem. Phys. 32, 843 (1960).

101. N. Itoh, B. S. H. Royce, and R. Smoluchowski, Phys. Rev. 138, A1766 (1965).

102. T. P. P. Hall, D. Pooley, W. A. Runcinam, and P. T. Wedepohl, Proc. Phys. Soc. (London) 84, 719 (1964).

103. D. Pooley and W. A. Runcinam, Solid State Comm. 4, 351 (1966).

104. J. D. Gibson, A. N. Goland, M. Milgram, and G. H. Vineyard, Phys. Rev. 120, 1221 (1960).

105. T. P. P. Hall, D. Pooley, and P. T. Wedepohl, Proc. Phys. Soc. (London) 83, 635 (1964).

106. R. O. Vilu and M. A. Elango, Soviet Phys.--Solid State 7, 2967 (1966).

107. J. D. Comins and P. T. Wedepohl, Solid State Comm. 4, 537 (1966).

108. C. J. Delbecq, W. Hayes, and P. H. Yuster, Phys. Rev. 121, 1043 (1961).

109. F. J. Keller and R. B. Murray, Phys. Rev. 150, 670 (1966).

110. G. L. Clark (ed.), The Encyclopedia of X Rays and Gamma Rays. New York: Reinhold Publishing Corporation, 1963, p. 1105.

111. J. E. Aguiar, "Design Criteria to Increase the Sensitivity of the Total Absorption Calorimeter for Soft X Rays." Unpublished M. S. dissertation, Department of Nuclear Engineering, University of Puerto Rico, Mayaguez, Puerto Rico, 1966.

112. F. Rosa, "Calibration of a Total Absorption Calorimeter for Soft X Rays." Unpublished M. S. dissertation, Department of Nuclear Engineering, University of Puerto Rico, Mayaguez, Puerto Rico, 1966.

113. A. Smakula, Z. Physik $\underline{59}$, 603 (1930).

114. Reference 47, p. 57.

115. Reference 47, pp. 77 and 103.

116. Reference 48, p. 33.

117. W. J. Veigele and N. J. Roper, J. Appl. Phys. $\underline{37}$, 4309 (1966).

118. R. B. Murray and F. J. Keller, Phys. Rev. $\underline{137}$, A942 (1965).

119. A. H. Compton and S. K. Allison, X Rays in Theory and Equipment. New York: D. Van Nostrand Company, 1943.